ADVANCED ANTIREFLECTIVE COATINGS FOR POLYCARBONATE SUBSTRATES

THESIS

Presented to the Graduate Council of
Texas State University-San Marcos
in Partial Fulfillment
of the Requirements

for the Degree

Master of SCIENCE

by

Jeffrey R. Simpson, B.S.

San Marcos, Texas
August 2013

ADVANCED ANTIREFLECTIVE COATINGS FOR

POLYCARBONATE SUBSTRATES

Committee Members Approved:

Chad J. Booth, Chair

Donald E. Patterson

Todd W. Hudnall

Luyi Sun

Approved:

J. Michael Willoughby
Dean of the Graduate College

FAIR USE AND AUTHOR'S PERMISSION STATEMENT

Fair Use

Duplication Permission

DEDICATION

Dedicated to my loving wife Molly

Thank you for your support

ACKNOWLEDGEMENTS

This work was supported by Air Force STTR Phase I Contract No. FA9550-12-C-0005. The author would like to thank the Welch foundation for funding under the Texas State University-San Marcos Graduate Summer Research Fellowship 2012 from The Welch Foundation Departmental Research Grant Program Al-0045. Nanohmics, Inc. contributors to be recognized are Don Patterson, Mike Mayo, Byron Zollars, Mike McAleer, Dan Mitchell, Rey Guzman, Ron Sullivan, Roger Wood, and Kyle Hoover. Thesis committee members to be recognized for significant constructive input are Don Patterson, Todd Hudnall, Luyi Sun, and most of all Chad Booth.

This manuscript was submitted on July 8, 2013.

TABLE OF CONTENTS

Page

LIST OF TABLES

Table **Page**

LIST OF FIGURES

Figure **Page**

LIST OF ABBREVIATIONS

Abbreviation	Description
AFM	Atomic Force Microscopy
AR	Antireflective
ARC	Antireflective Coating
DOE	Design of Experiment
Er:YAG	Erbium: Yttrium Aluminum Garnet
FTIR	Fourier Transform Infrared Spectroscopy
HMDS	Hexamethyldisiloxane
HSP	Hanson Solubility Parameters
IR	Infrared
LN2	Liquid Nitrogen
MAK	Methyl Amyl Ketone
MALDI	Matrix Assisted Laser Desorption Ionization
MAPLE	Matrix Assisted Pulsed Laser Evaporation
MEK	Methyl Ethyl Ketone
Nd:YAG	Neodymium: Yttrium Aluminum Garnet
nm	Nanometer
NRL	Naval Research Laboratory
NRLP	Naval Research Laboratory Polymer

PC.....Polycarbonate

PFH .....Perfluorohexanol

PLD ..... Pulsed Laser Deposition

PMMA ..... Polymethylmethacrylate

RIR-MAPLE ..... Resonant Infrared Matrix Assisted Pulsed Laser Evaporation

STTR..... Small Business Technology Transfer

TAF .....Teflon® AF

TGA ..... Thermogravimetric Analysis

THF ..... Tetrahydrofuran

UV ..... Ultraviolet

UV-MAPLE .....Ultraviolet Matrix Assisted Pulsed Laser Evaporation

CHAPTER 1

BACKGROUND

Antireflective Coatings

In today's world the need for specialized materials has never been greater. Material properties which are specifically suited for a certain application require extensive research for refinement of those desired properties. One such desirable material property is the control of surface reflection. When light passes from one medium with a given refractive index, determined by the ratio of the speed of light in a vacuum to its speed in the medium, to another with a different refractive index, some light does not traverse the interface and is reflected. The magnitude of this reflection is dependent on the wavelength of the light, the angle at which the light encounters the new medium and the relative refractive indices of the media at the interface. Reflections can reduce the effectiveness and efficiency of many light emitting and transmitting devices. Antireflective coatings (ARC) have been developed through a variety of methods to both reduce reflection and increase transmission across a given interface. Antireflection is achieved by two general designs: parallel surface coatings aimed to reduce reflection of specific wavelengths and modification of surface morphology which increases the surface area of an interface which significantly affects the angle of incidence and acts as a refractive index gradient. The former is optical thickness dependent and the latter is morphology and refractive index dependent.[1] Surface morphology ARCs originated in

nature. The stereotypical example of such a coating is the eyes of moths. Moth eyes are covered with sub-wavelength nipple-like protrusions that act as a refractive index gradient, minimizing reflection and detection by predators.[1]

The simplest parallel surface ARC model is the quarter-wave interference coating. This single layer coating on a reflective surface is designed to minimize the reflection of a given wavelength. Light that passes through this coating will travel to the reflective surface and be reflected back through the coating. The total distance traveled by the light in the coating must be equal to one half of the light's wavelength. Light that is reflected off of the coating surface will interfere destructively with the light that was reflected off of the interior surface of the coating. This scenario is shown in Figure 1. This destructive interference occurs because the two light paths create light that is perfectly out of phase, effectively cancelling out any intensity. More complicated modeling is necessary to accomplish broader anti-reflection accommodating multiple wavelengths of light, refractive indices of materials, and multiple layer structures. These models are complicated and use sophisticated software.[2-4]

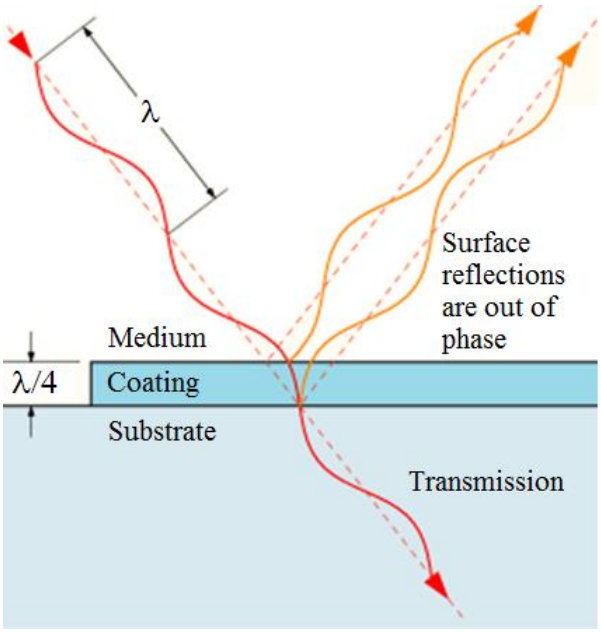

Figure 1. Destructive interference of out-of-phase reflections from the two interfaces of the quarter wavelength coating eliminate shared intensity, making the coating antireflective.

Antireflective coatings are used in a variety of applications. Optical equipment, such as eye glasses and camera lenses, are the most common use for these coatings. Examples of ARCs are shown in Figure 2.[1] Additional uses include improvement of transmission for solar cells, photolithography in microelectronics, glare reduction for display screens, and various military applications. Materials used for these coatings are typically inorganic oxides, nitrides and sulfides. Deposition methods for these and similar coatings also vary. Chemical bath, sol-gel, hot embossing, sputter coating, and spin coating are just a few deposition methods used in antireflective films.[1,4-8] Unfortunately, eye glasses and many other optical windows are often made of polycarbonate and similar polymers whose coefficients of thermal expansion differ greatly from these inorganic coatings. Polycarbonate has a linear thermal expansion coefficient of 68 x 10^{-6}/°C[12] while a commonly used antireflective coating for eyeglasses,

MgF_2, has a coefficient of 13.7 x 10^{-6}/°C.[10] This approximately five fold difference results in stress at the substrate coating interface. Mechanisms for relief of this stress cause failure of the optical properties of the coating. Common relief mechanisms are cracking or crazing and delamination of the film.

Figure 2. Antireflective coatings reduce glare and improve optical acuity.[1]

Alternatives to these inorganic films have been investigated.[11-13] Nanostructured arrays of close packed 200-300 nm sized cones have been produced to mimic the antireflective nature of moth eyes. A compact arrangement of small, sub-wavelength, cones or pillars prevent reflection by being individually smaller than the wavelengths of visible light, too small to reflect those wavelengths. The array effectively creates a smooth transition of refractive indices between the medium and the moth eye structure, preventing reflection and maximizing transmission to the substrate. Given that these structures are not a concise film, but rather an arrangement of individual pieces, they are not subject to crazing like inorganic films. The primary drawback to these nanostructured layers is that they are incredibly fragile and can be damaged or removed easily. The need exists for an ARC with a coefficient of thermal expansion comparable

to its substrate. The opportunity exists to create a coating that is durable and compatible with polymeric lenses in an organic molecule deposition process called MAPLE.

Matrix Assisted Pulsed Laser Evaporation (MAPLE)

Originally developed in the 1990's by Dr. James Griffith at the Naval Research Laboratory[14] as an alternative form of Pulsed Laser Deposition (PLD), Matrix Assisted Pulsed Laser Evaporation (MAPLE) has become a widely utilized technique for thin film deposition by laser ablation. The MAPLE deposition process is superior to traditional PLD techniques for use in organic film deposition. This superiority stems from the high degree of preservation of the deposited material's chemical structure and molecular weight.[15] Pulsed laser depositions range from high power pyrolytic chemical vapor depositions to low power ablative techniques like MAPLE. Even at low power, organic polymers and biomaterials tend to be vulnerable to photodegradation by traditional PLD techniques.[16] Tailoring the components of the MAPLE process to be compatible is very important. The interaction of the laser with the components of the matrix is the primary design factor which protects organic solutes and will be discussed below.

Generally, MAPLE systems require specific components for operation. The laser, the matrix and the substrate are highly variable across processes and are responsible for film quality. All processes start with a laser as a light source for evaporation of the solid matrix target. Lasers typically have a small operable temperature window. Cooling systems are used to maintain a constant temperature ensuring a constant laser power output. Various mirrors, lenses, and transparent windows are used to direct the beam into the low pressure chamber where it is focused on the target surface. The target matrix

must be constantly cooled to sustain a frozen solid state. The preservation of a solid target is essential for the deposition mechanism which relies on a solid to vapor transition for formation of an energetic plume, ejecting matrix solutes. Additionally, targets may be held vertically and would fail to remain in the laser's path if the matrix melted. Cooling methods vary slightly but typically consist of a liquid nitrogen cooled base which holds the target. Alternative cooling methods, for systems which need a mobile target, may incorporate a bellow to push cooled air through the target base.[17] Once excited by the laser, the target matrix solvent molecules vaporize to form the energetic plume normal to the surface of the target, as seen in Figure 3,[18] carrying with it any non-solvent or non-volatile molecules. Deposition conditions within the chamber are system specific but generally, the chamber is pumped down to very low pressures so to effectively clear the solvent vapor.

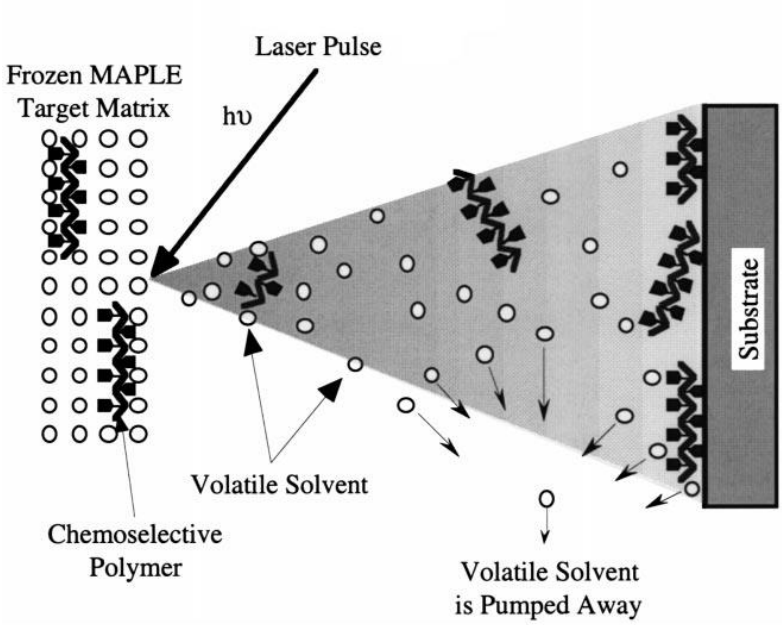

Figure 3. Energetic plume of vaporized solvent molecules from the matrix eject solutes onto the substrate.[18]

Chamber pressure is variable across MAPLE processes. Pressures can range from

10 mTorr to just under atmospheric pressure.[14] Deposition conditions are reached using a high vacuum pump down and back fill of a dry inert gas. The substrate is often heated to encourage film uniformity through further evaporation of any residual solvent molecules resulting in relaxation of deposited polymer strands which can improve film quality.[19] Homogenous vaporization and uniform deposition are essential to a reliable deposition process. The conditions at the laser-matrix interaction site on the target surface must be consistent with each pulse. Methods to achieve this include slow rotation of the target matrix, or rastering the incoming beam through the programmed motions of a motorized mirror prior to entering the chamber. The chamber must be at very low pressures to encourage the solvent vapor clearance prior to reaching the substrate. Molecules which are not in a gas phase that have enough velocity from the plume will deposit on the substrate which is centered directly above the laser-matrix focal point at an experimentally determined distance. Ambient gas used to fill the chamber must be free of moisture or other contaminants that could condense on the frozen matrix surface, interfering with laser-matrix interaction, nitrogen gas is commonly used. Ice or other contaminant particle layers on the target surface can interfere with the absorbance of the light by the solvent matrix,[14] thereby decreasing the volume and velocity of the ejected plume, and result in unwanted debris on the substrate. The most important differentiating equipment from one MAPLE system to the next is the laser.

Laser variation in MAPLE systems segregates processes into two main categories: ultraviolet (UV) and infrared (IR) wavelength emitting lasers. The former is more traditional and typically more powerful, given the higher energy wavelength. Lasers capable of emitting in the ultraviolet, such as the Excimer or Nd:YAG lasers, are

commonly used in MAPLE processes which deposit inorganic materials. These lasers are well suited for matrices whose solvent molecules are generally transparent to visible and infrared wavelengths.[20,21] Infrared lasers are more appropriate for large organic molecules whose potential degradation would be detrimental to the deposition process and film quality. The infrared subset of MAPLE processes has been dubbed Resonant-Infrared MAPLE (RIR-MAPLE).[14,15,22]

The benefits of RIR-MAPLE over more traditional UV-MAPLE processes center on the ability to maintain structural integrity of large organic molecules, including biomolecules and polymers. This ability is due to the selective absorbance of certain matrix constituents. As the name implies, these molecules have bonds that are highly receptive to absorbing the specific IR wavelength, thereby "resonating." Specific to this work, the Er:YAG laser emits at 2937 nm which corresponds to ~3405 cm^{-1}. Common organic functional groups which absorb this wavelength are amines and alcohols, specifically the N-H and O-H bonds of these functional groups. The higher the concentration of these bonds, the higher the absorption by the matrix. As an aside, a popular additive into RIR-MAPLE matrices is water.[23] Water absorbs the IR wavelengths very well as it essentially consists of two O-H bonds per molecule. A potential limitation for the use of water in MAPLE matrices is the solubility of the deposition solutes in water or a cosolvent system containing water.[24]

The mechanism driving the RIR-MAPLE deposition process is the laser-matrix interaction. Generally described as an ablation, the interaction is more appropriately called explosive boiling.[25] The mechanism involves absorption followed by an ejection of mass from the target. The fluence (laser energy per unit area), coupled with the degree

of absorption, determines the effectiveness of the mechanism. A fluence threshold has been shown to exist, above which effective mass ejection occurs, below which the energy is transferred and is not sufficient to vaporize matrix solvent molecules and may instead melt the matrix.[25] Direct application of the fluence threshold to RIR-MAPLE encourages the conclusion that a very high fluence will produce the maximum ejection of material. Depending on the criteria used to evaluate the film, maximizing deposition rate may be ideal; however, in practice, increased deposition rate and increased film quality are not synonymous, especially when roughness is an evaluation metric. Another ablative technique that is widely used is the Matrix Assisted Laser Desorption Ionization (MALDI) technique for mass spectrometry. MALDI's mechanism is also based on the laser-target interaction except the process goal is to ionize and break apart the solute molecules for characterization in a time of flight device. Similar, but technically opposite from MALDI, MAPLE utilizes a solvent matrix to absorb light for a gentle deposition of large molecules ejected with a plume of volatilized solvent. Leaving the solute molecules intact is the key difference between the two. A strong similarity between the techniques is the formation of the matrix and its importance in the success of each process.[26]

While the laser-matrix interaction is the mechanism that determines the effectiveness of deposition, the composition of the matrix determines film quality and is the most important design criterion in MAPLE thin-film deposition. The desired deposition material will naturally limit the solvents available for matrix composition. The first thing to consider when choosing solvents is the solubility of the solute molecules. The second is the solvents' IR absorbance spectra corresponding to the laser-matrix interaction. While many polymers and biomolecules are soluble in a variety of

solvents, not all solvents sufficiently absorb an IR wavelength of 2937 nm. As previously stated, an obligatory component for the matrix is a high concentration of O-H or N-H bonds to facilitate this absorption. Many potential deposition molecules are not directly soluble in alcohols or amines. Solvent systems comprising of two or more solvents are often used to satisfy both basic needs of the matrix solvents: solubility and absorbance. Binary or ternary solvent systems may be used, however due to the frozen nature of the matrix, cosolvent systems may be difficult to use. A significant concern for polymer solutes used in MAPLE deposition is the potentially differing polarities between the non-polar polymer backbone and polar pendant groups. Cosolvent systems may satisfy both regions successfully. Ideally, a given polymer molecule will not interact with another in a MAPLE solution or matrix. If polar pendant groups, such as the methacrylate group in polymethylmethacrylate (PMMA), are not solvated, then those polar regions will tend to cluster and segregate themselves from nonpolar solvents. If these polymer clusters exist in the matrix, they will also exist in the deposited layer as seen in the scanning electron microscope image in Figure 4.[27] The images are of PMMA that has been forced to cluster in toluene. The MAPLE process that produced these images used an ultraviolet light source. To remedy this clustering, addition of a second solvent to toluene is necessary; this binary system and its resulting films will be discussed below.

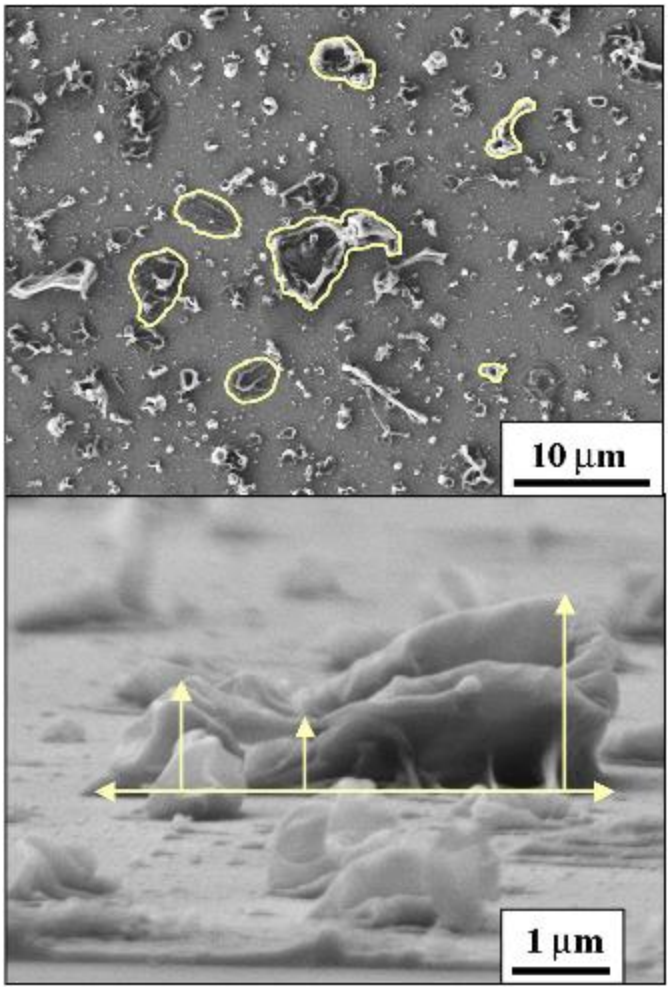

Figure 4. PMMA clusters present on a deposited MAPLE film.[27]

Solubility is generally determined at room or elevated temperatures; however the MAPLE matrix must be frozen to be effective. Any liquid solubility issues will be greatly pronounced when the temperature of the solution drops. A polymer solute that drops out of solution prior to freezing will deposit as large strands instead of a concise film, as shown in Figure 5. This is due to exclusion from the freezing solution and non-uniform precipitation throughout the frozen matrix.

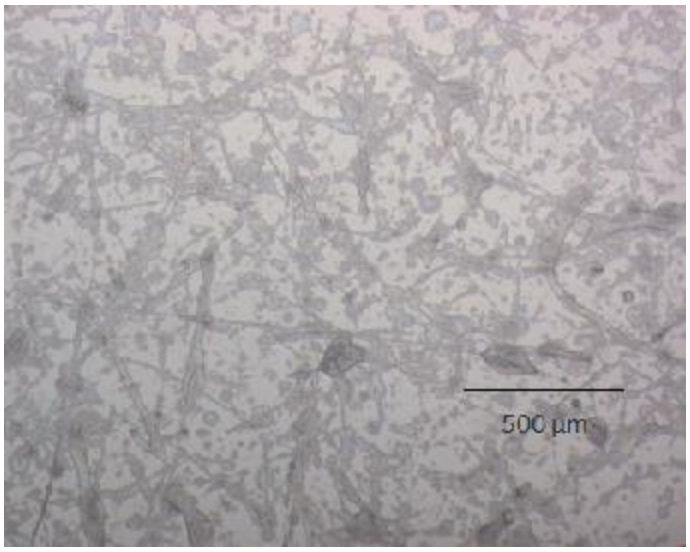

Figure 5. Polymer strands present on a MAPLE-deposited film due to solubility limitations.

Maximizing the liquid solubility of a given polymer in its solvent system is a method used to encourage homogeneity in the solid matrix. The weight percent of the dissolved polymer in MAPLE matrices are typically very low, generally well below ten percent and for many processes below one percent. These concentrations are often within the solubility limits of the solution at room temperature. Efforts to change binary solvent ratios in order to maximize the solubility of the polymer increase the likelihood that the polymer will stay in solution when freezing. One such model for maximizing solubility is the Hansen Model.[28] The Hansen Solubility Parameters (HSP) attribute values to physical parameters: dispersion forces, polarity and hydrogen bonding. The three parameters act as three dimensional coordinates which, with some mathematical adjustment, represent a sphere of solubility for a given polymer. If a solvent's parameters are within a polymer's solubility sphere then it is likely to have a favorable interaction. For binary solvent systems, the HSP can be represented graphically as the solubility radius of the solution versus the mole fraction of a solvent in the system as shown in

Figure 6.[29] This graph represents the ideal mole fraction of toluene needed to maximize PMMA solubility in a binary toluene:methanol solution. As mentioned above, the solvent components of this binary solution both contribute to the solubility of the polymer. The methanol better solvates the methacrylate pendant groups of the PMMA allowing the groups to segregate and disperse evenly. For RIR-MAPLE, the methanol serves a second vital role of having absorbance at 3405 cm^{-1} facilitating the MAPLE deposition mechanism.

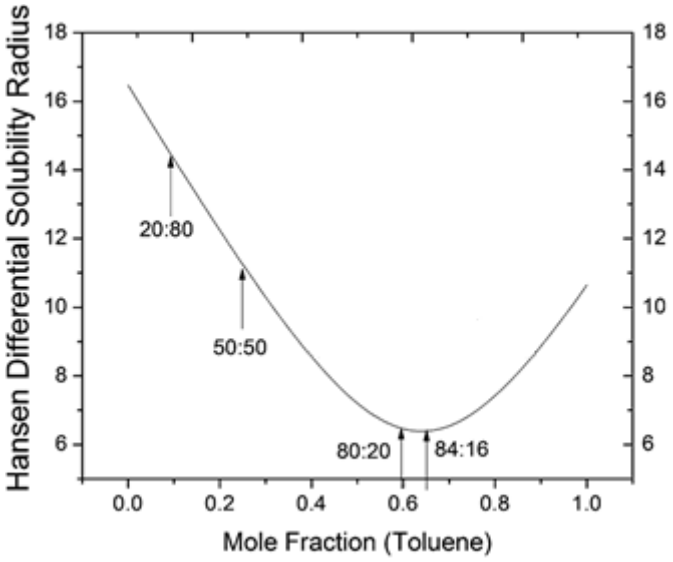

Figure 6. Hansen Solubility Radius versus mole fraction of toluene in a binary toluene:methanol solution. This is specific for PMMA.[29]

Liquid miscibility of solvents and maximization of solute solubility in a given system are important factors to consider to encourage good film quality for the RIR-MAPLE process. Binary solvent systems are useful to satisfy the needs of a solvent matrix, primarily solubility and absorbance. A secondary consideration that will likely not be evident until a matrix is prepared from a given solution is the solid solubility of the solvents. While at very low concentrations, a solute will most likely not affect the

preferred phase arrangement of the matrix. The solvents in a binary system, however, will likely be at high enough concentrations to have significant impact on the phases of the matrix. Eutectic phase diagrams are very valuable when designing these matrices, but for many organic solvents these diagrams are not available in literature. The spectrum of matrix quality that comes from binary systems has significant impact on the deposition process and film quality. The images in Figure 7 illustrate the differences in matrix appearance from solvent systems. The center image is the most common appearance for a system where two solvents are both significantly represented. The left and right images represent the ends of the appearance spectrum and entail dramatic differences for RIR-MAPLE performance and film quality. The image on the left is a ternary PMMA solution comprised of toluene, methanol and tetrahydrofuran (THF). The THF was added as an intermediate solvent between toluene and methanol in hopes to improve compatibility and therefore homogeneity of the frozen matrix. The resulting MAPLE process only served to melt the relatively transparent matrix. The central image is the binary PMMA solution of toluene and methanol mentioned above. It is not suitable for MAPLE deposition due to partial transparency and heterogeneous regions of non-absorbent toluene. The image to the right is a binary fluorinated polymer solution of methyl ethyl ketone and methanol. This matrix appearance is ideal for MAPLE deposition due to its thermal stability and homogeneity. MAPLE deposition of this system will be discussed later.

Figure 7. Possible conformations of frozen matrices of solvent systems. The matrix to the left is essentially non-ordered and is likely to be poorly absorbing. The center matrix has segregated into two phases. The matrix on the right is the ideal homogenously frozen solution for the MAPLE deposition process.

The quality of the film that is produced by the RIR-MAPLE process, depending on the specific evaluation criteria, drives the need to fine tune matrix components. In this work, the optimization of film transmission is the driving evaluation criterion. The primary factor effecting transmission is film roughness. Reducing film roughness is a common effort in MAPLE research.[30-32] There are two matrix properties that have been directly linked to film roughness and therefore quality. The first has been implied in the preceding paragraphs: the segregation and dispersion of the solutes. This is the consequence of the first primary role of a matrix solvent, namely solubility. The second primary role is absorbance and is appreciated in the matrix property of laser penetration depth or, restated, the energy absorbed per matrix volume resulting in ablation and mass displacement. Maximizing matrix homogeneity and energy absorbed per matrix volume simultaneously is the solution to the roughness problem. A simple solution to matrix homogeneity is to allow the matrix to freeze in as small a volume as possible repeatedly, eventually forming a target sized volume. This procedure is tedious and difficult to

employ in practice due to the amount of time required to drip and distribute the solution into the target holder. The more repeatable and commercially feasible method for matrix homogeneity lies in tailoring the matrix solvents to behave ideally when freezing.

The source of roughness of the MAPLE process comes from the tendency of the ejected volume to aggregate to form bubbles or droplets en route to the substrate surface. These droplets are responsible for solvent retention and when deposited will contribute to the roughness of the film. Modeling to compare energy densities per ejection has been carried out.[33] Figure 8 illustrates the diversity of forms these deposited droplets can take. Black regions in Figure 8 represent retained solvent molecules. Shown in Figure 9,[29] the roughness of the droplets is significant and is a consequence of solvent retention increasing as polymer concentration increases. This is mostly intuitive. As the polymer concentration increases, the likelihood of polymer-polymer interaction is increased which deviates from the ideal model of single molecule deposition.

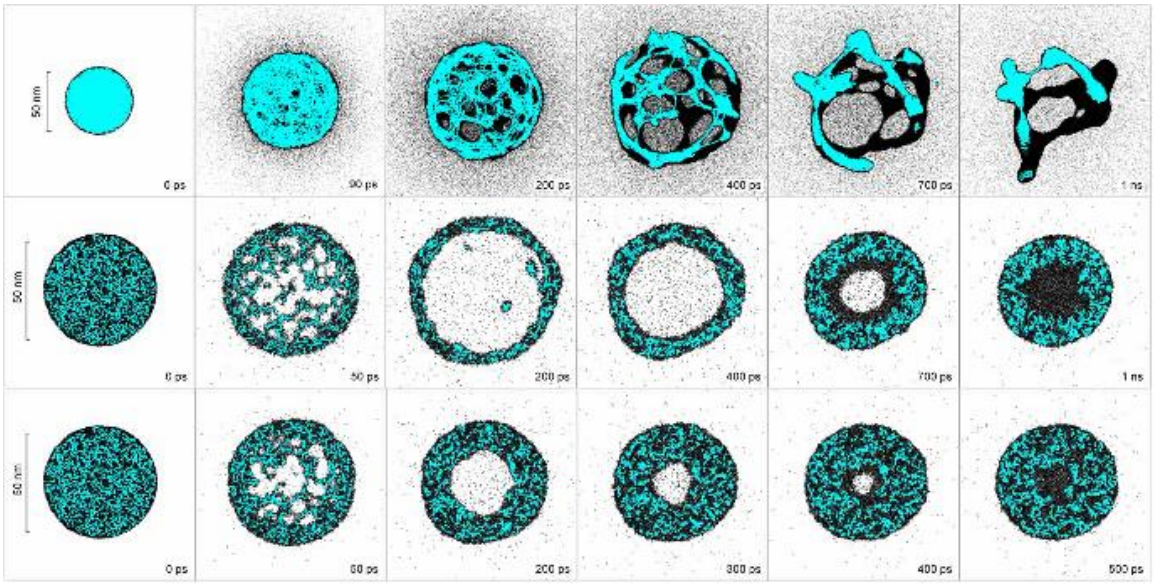

Figure 8. Modeled droplets or bubbles formed by ejected polymer from a MAPLE process. Images vary with laser excitation times and polymer concentrations.[33]

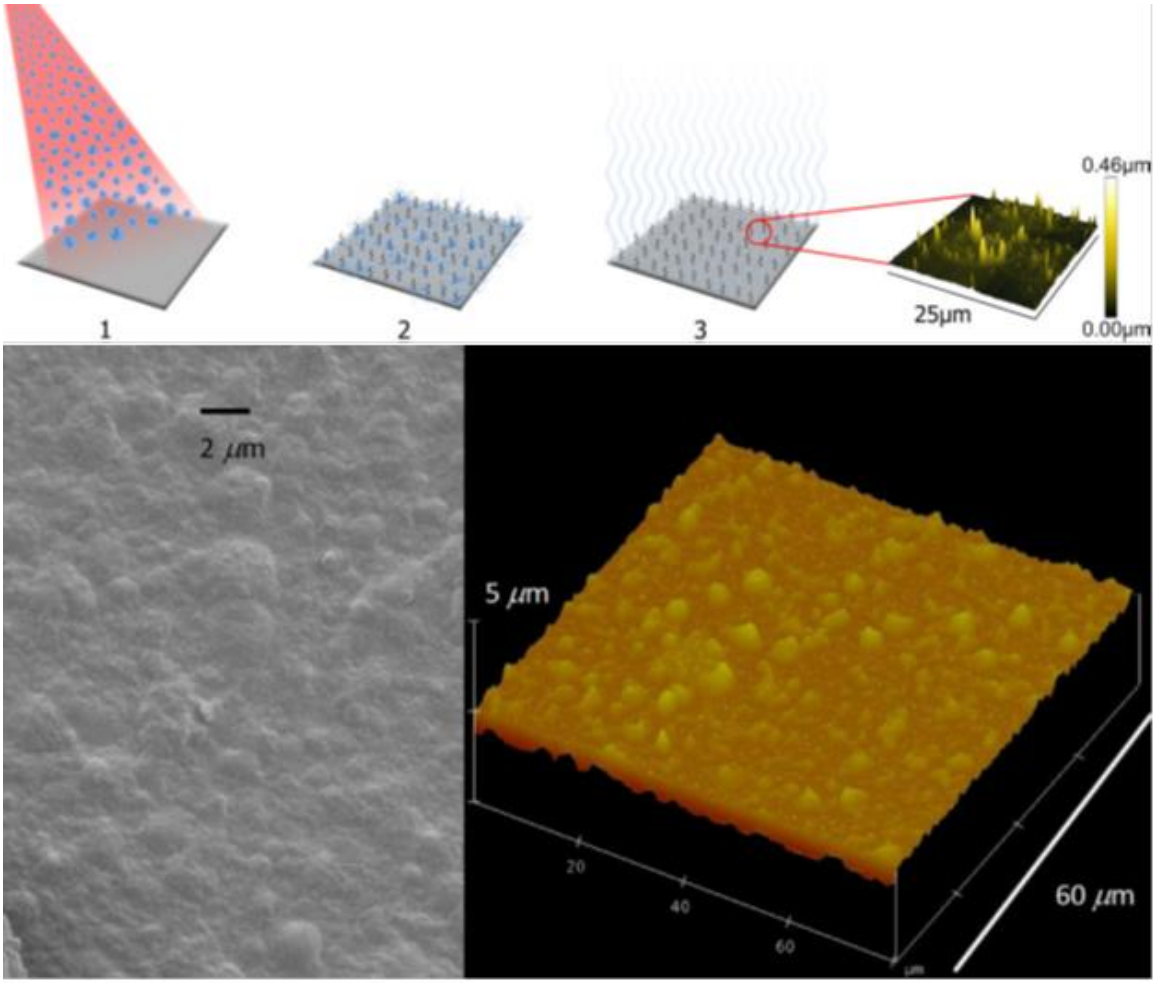

Figure 9. Roughness of MAPLE deposited films is attributable to polymer aggregation and solvent retention. The top images show the consequence of solvent retention. The bottom left image illustrates the prevalence of bubbles on the surface. The bottom right AFM image qualifies roughness across a given MAPLE-deposited surface.[29]

The need exists for an ARC for polymer substrates that is adherent, durable, and most of all has a compatible coefficient of thermal expansion to avoid typical failure mechanisms associated with common inorganic ARCs. Using MAPLE as an organic molecule deposition process, a thin ARC should be attainable. Development of the deposition process and design of the ARCs are discussed in Chapter 2.

CHAPTER 2

PROSPECTUS

The work described herein initiated from the Air Force STTR program, topic number AF10-BT19, entitled "Organic & Hybrid Organic/Inorganic-Based Graded-Index/Layered Optical Coatings by Physical Vapor Deposition."[34] The purpose of the project is to address the issues commonly found in antireflective coatings, specifically the mismatch of coefficient of thermal expansion between substrates and coatings which results in stress at layer interfaces causing failure of optical properties, most commonly seen as cracking or delamination. The terminal goal is to develop an environmentally durable adherent antireflective coating for polycarbonate flats using organic or mixed organic/inorganic layers. Organic layers are to be deposited by a physical vapor deposition process such as the pulsed laser deposition (PLD) derivative, MAPLE. Benefits of the MAPLE deposition technique include: preservation of chemical structure of deposited molecules, precise thickness control necessary for antireflective properties, and consistent film thickness. These MAPLE-grown layers will be part of layered structures designed according to mathematical models.

Mathematical modeling prescribes layer combinations of material thickness and refractive indices designed to reduce broad band reflection. Target goals are a transmission greater than 99.5% and reflection less than 0.5%, for a 400 nm – 750 nm passband. Once deposited, coatings will be evaluated by spectroscopic ellipsometry for

adherence to the prescribed models and their optical parameters. The work will ultimately produce a thin-film fabrication process that is reproducible and controllable. Final environmental testing will adhere to military specification MIL-C-48497A.

Development of the MAPLE deposition process is the primary focus of this project. This will include system construction and determination of deposition parameters. Materials to be used for deposition including matrix solvent(s) and deposition polymer(s) will be established. Solvents will absorb irradiating light effectively for deposition mechanism and the polymers will be appropriate for antireflective coatings. Films will be deposited on glass, silicon, and polycarbonate substrates using a combination of MAPLE and magnetron sputtering. Films will be structured according to mathematically modeled prescriptions to minimize reflection and maximize transmission. These coatings will be characterized using optical microscopy to gauge surface quality, ultraviolet-visible spectroscopy to measure reflection and transmission, and interferometry to verify layer thicknesses. Characterization will confirm film adherence to the prescribed model. Environmental testing will establish coating durability.

CHAPTER 3

MATERIALS AND METHODS

Optical Modeling

Before modeling ARCs, optical constants needed to be obtained for the coating materials. Thin films of PMMA, Teflon® AF, another fluorinated polymer to be discussed below, SiO_2, and AlN were deposited to obtain these constants. A 1 wt% solution of PMMA (Sigma-Aldrich) in CH_2Cl_2 (VWR) was spin-coated onto a Si wafer (University Wafer, 50.8 mm diameter, p-type, B-doped, single side polished) using a Laurell Technologies spin coater (Model no. WS-400B-6NPP/LITE). Before coating, the Si wafer was pretreated with hexamethyldisiloxane (HMDS; MicroChem) to promote adhesion of organic molecules through the addition of trimethylsilane groups to the surface of the wafer. A spin speed of 5000 rpm for 60 seconds was used for both of the spin coatings. The PMMA film was hard baked onto the Si wafer by heating it at 100 °C for 60 seconds. The film thickness was measured using a Dektak 150 profilometer. The optical constants were obtained using a Woollam M-2000-DI ellipsometer and yielded the dispersion curve shown in Figure 10. A Cauchy fit[35] was applied to the data and the Cauchy coefficients are given in Figure 10.

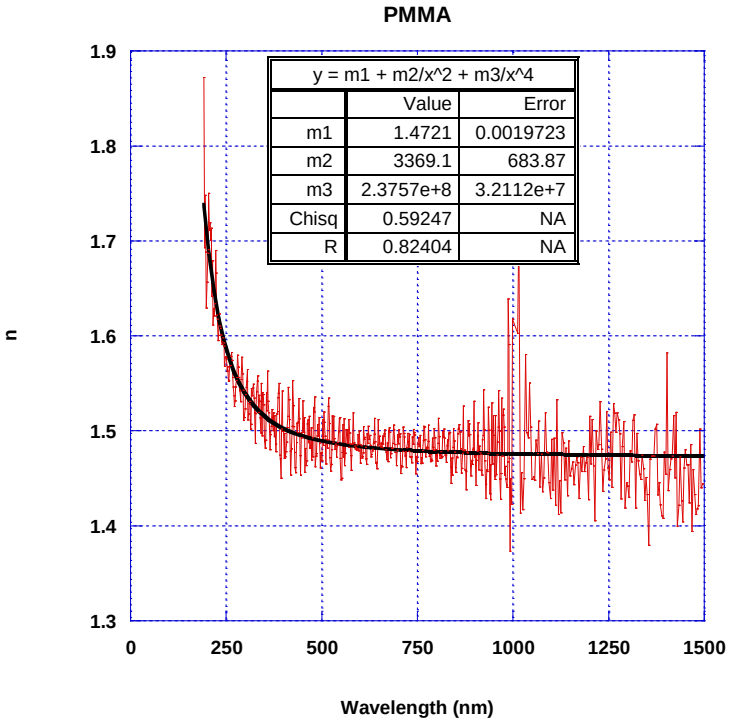

Figure 10. Dispersion curve for thin film Polymethylmethacrylate (PMMA) on Si. The Cauchy fit and constants are shown in black.

Similarly, a HMDS pre-treated Si wafer was spin coated with a 1 wt% Teflon® AF solution (DuPont™; Grade 400S2-100-1). This solution contains 1% Teflon® AF, copolymer of 2,2-bistrifluoromethyl-4,5-difluoro-1,3-dioxole, shown in Figure 11, in perfluorinated solvent C5-18.

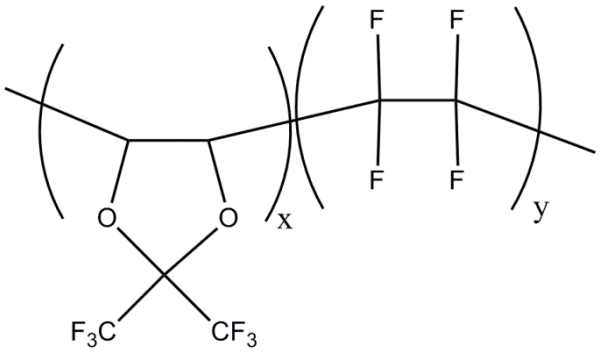

Figure 11. Molecular structure of Teflon® AF.

Teflon® AF has the potential of being a superior optical coating due to its low index of refraction and good optical transparency.[36,37] As with the PMMA coating, the Teflon® AF was spun on a HMDS treated Si wafer at 5000 rpm for 60 seconds, followed by hard baking at 100 °C for 60 seconds. The thickness of the film was again measured by profilometry. The dispersion curve for Teflon® AF, Figure 12, shows a very low index of refraction from 400 to 750 nm.

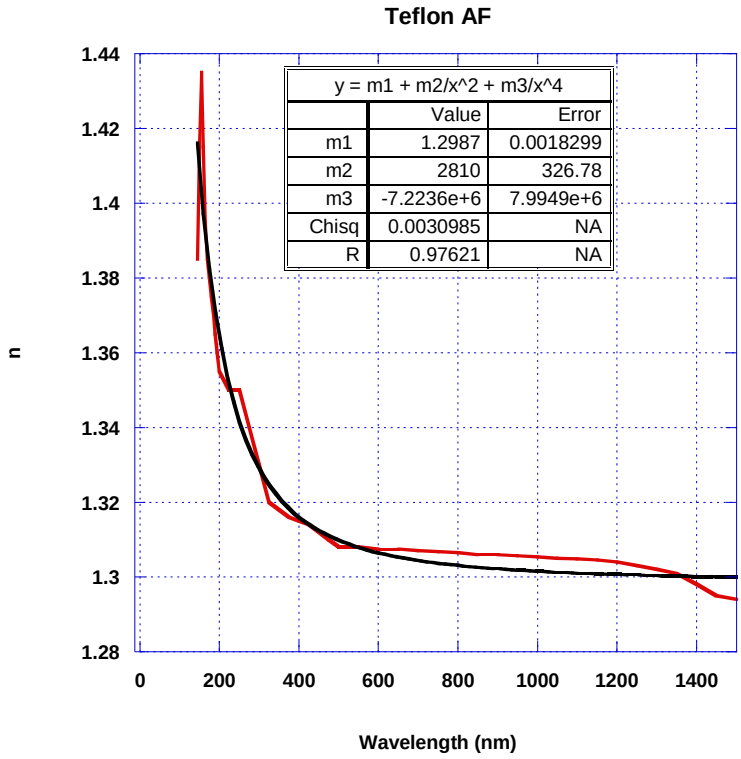

Figure 12. Dispersion curve for thin film Teflon® AF on Si. The Cauchy fit and constants are shown in black.

Finally, another fluoropolymer to be investigated, NRL polymer (NRLP), (70% solution in methyl amyl ketone (MAK); ExFluor, Inc. Figure 13) was spun onto Si and prepared in an analogous manner to that for the Teflon® AF. The NRLP's dispersion curve is shown in Figure 14. The NRL polymer was originally developed at the Naval

Research Laboratory as an adherent, anti-corrosion layer and has now found numerous uses including fuel tank linings, marine anti-fouling coatings, and de-icing layers.[38] Due to the polymer's superior adhesion and low index of refraction, the compound could prove to be a useful optical coating material.

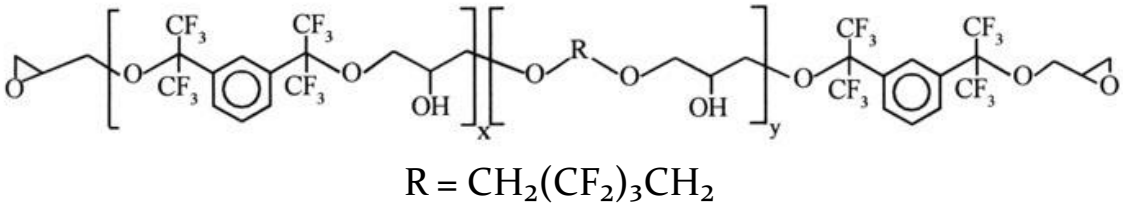

Figure 13. Molecular formula for the NRL polymer.

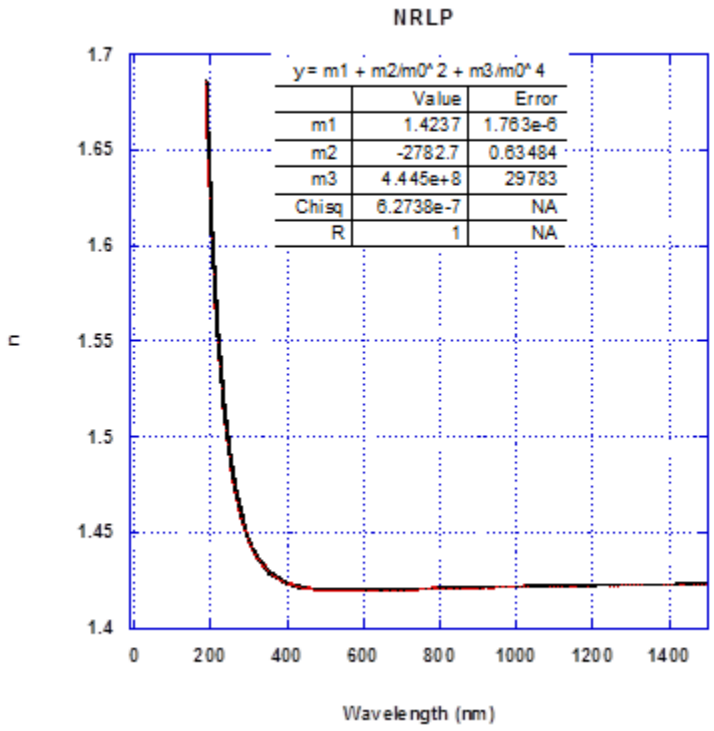

Figure 14. Dispersion curve for thin film NRL polymer on Si. The Cauchy fit and constants are shown in black.

AlN and SiO_2 were reactively sputtered onto Si wafers using a magnetron sputtering system. AlN was deposited from an Al target (Kurt Lesker, 99.9%) in a 50:50 $Ar:N_2$ atmosphere using a power of 200 W and a deposition pressure of 5 mTorr. SiO_2 was similarly deposited using a Si target (Lesker; 99.99%), and the background gas mixture was 50:50 $Ar:O_2$. The thickness of both films was about 100 nm. The dispersion curves for both of these materials are shown in Figures 15 and 16**Figure** .

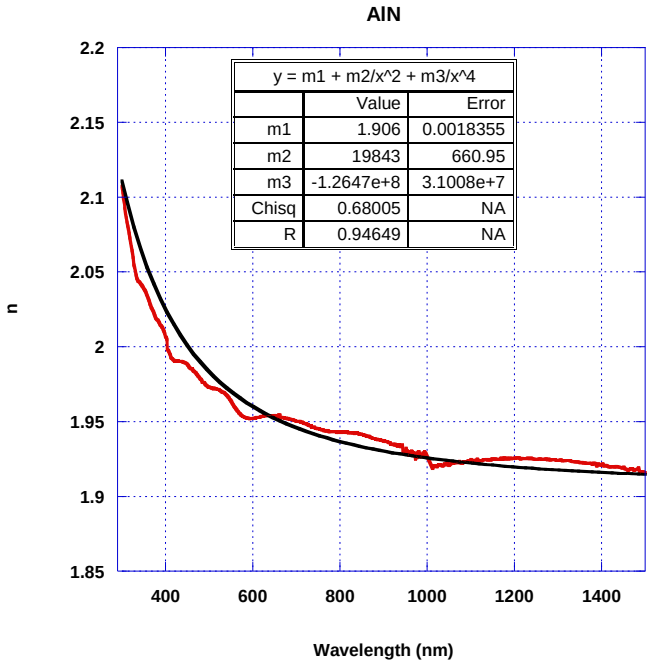

Figure 15. Dispersion curve for thin film AlN on Si. The Cauchy fit and constants are shown in black.

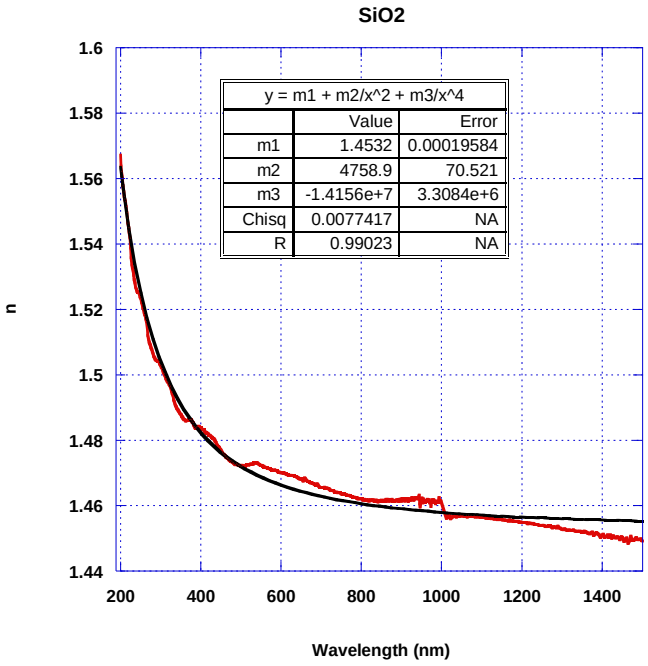

Figure 16. Dispersion curve for thin film SiO_2 on Si. The Cauchy fit and constants are shown in black.

Using the data from the dispersion curves, a model ARC of Teflon® AF on a polycarbonate (PC) substrate was produced. Modeling was performed using OpenFilters 1.0.2 software.[4] PC samples and dispersion curve data were obtained from SABIC Innovative Plastics (Lexan®; 3 mm thick). The target transmittance value is 1 with an error of 0.01 from 400 nm to 750 nm. The simplest prescription is given in Table 1: a two layer front surface coating and a single layer back surface coating. Addition of a thin protective layer of SiO_2 on the Teflon® AF layer has a minimal effect on the transmission of the PC. The theoretical transmission of the coated PC is shown in Figure 17 with the various stages of the coating process: SiO_2 only, SiO_2 + Teflon® AF on front surface, and the final complete coating. The front surface reflectance model is shown in Figure 18.

Table 1. Model prescription for a Teflon® AF based antireflective coating for polycarbonate.

Material	Thickness (nm)
Front	
SiO_2	261
Teflon® AF	100
SiO_2	10
Back	
Teflon® AF	100
SiO_2	10

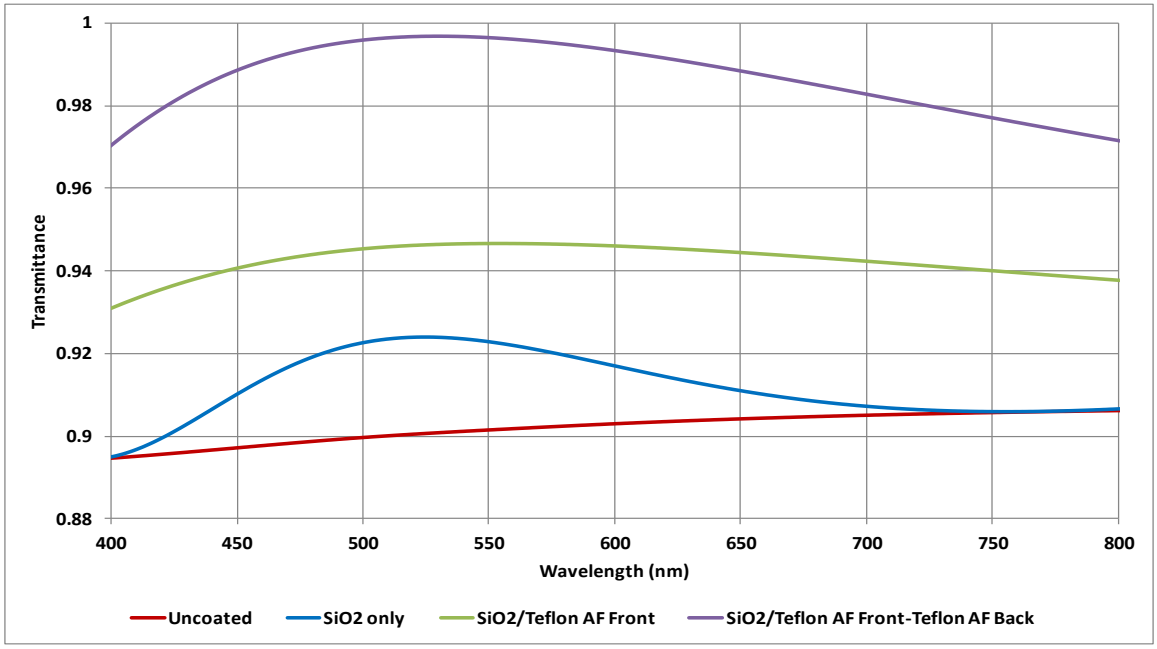

Figure 17. Model of the SiO_2/Teflon® AF AR coating for polycarbonate windows (top) and the schematic representation of the coating (bottom).

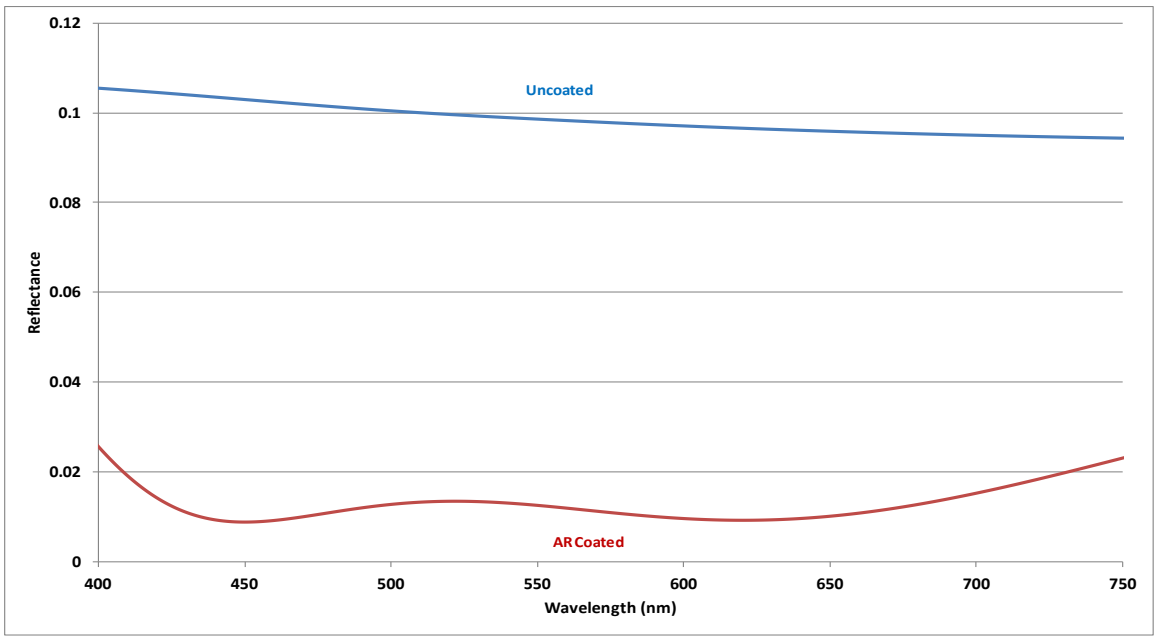

Figure 18. Reflectance model for the SiO_2/Teflon® AF AR coating for PC windows.

In order to develop the MAPLE process, an inexpensive polymer was needed, PMMA was modeled. To accompany the PMMA, AlN was chosen as an external layer because it is hard and inert. From ellipsometry data, modeled coating layers for the PMMA-based ARC are given in Table 2 and the resultant transmission model is given in Figure 19. Table 2 lists the values for both a 3-layer (each side) and 5-layer (each side) coating.

Table 2. Model prescription for a PMMA based antireflective coating for polycarbonate.

Material	Thickness (nm)
3-Layer Model	
Front	
AlN	30
PMMA	104
AlN	10
Back	
AlN	25
PMMA	115
AlN	10

(Table 2-Continued) Model prescription for a PMMA based antireflective coating for polycarbonate.

5-Layer Model	Thickness (nm)
Front	
AlN	124
PMMA	175
AlN	122
PMMA	91
AlN	10
Back	
AlN	118
PMMA	166
AlN	107
PMMA	74
AlN	10

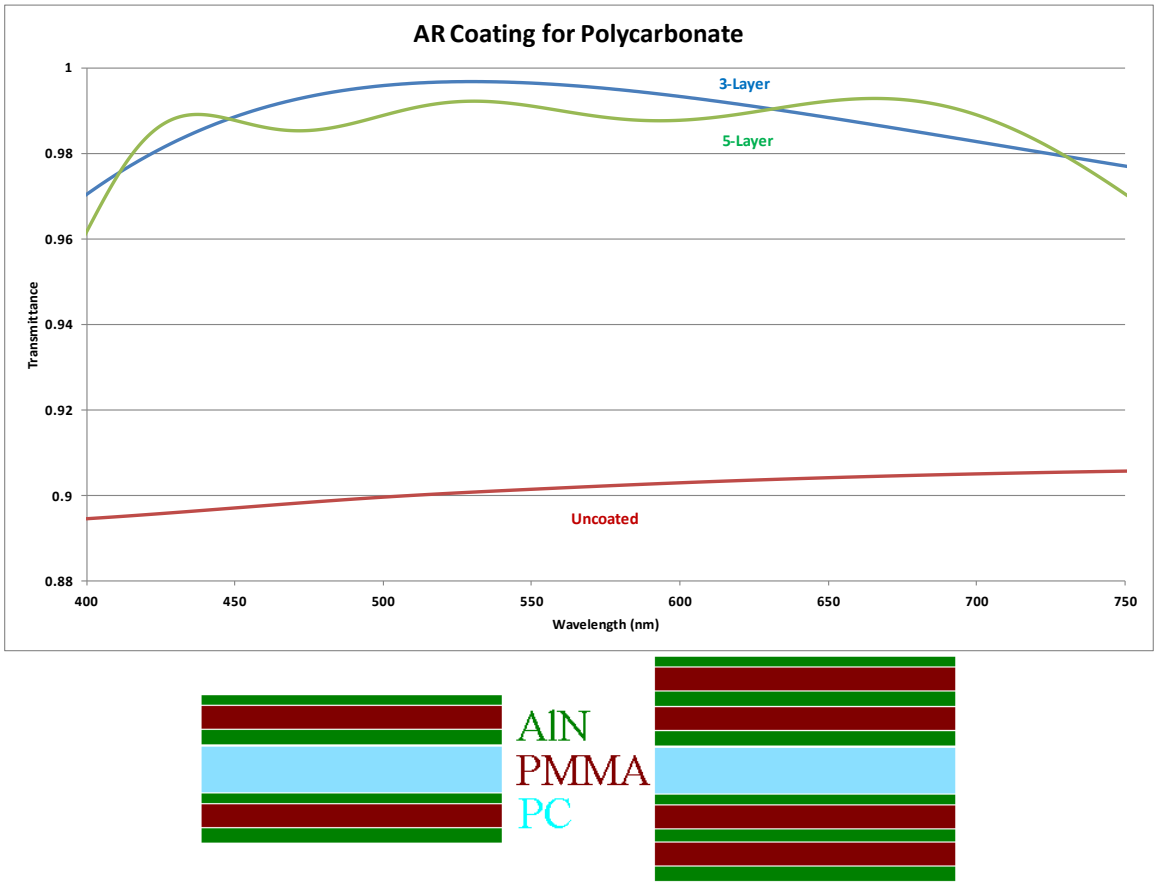

Figure 19. Modeled transmittance of an AR-coated PC window using prescribed stacks from Table 2 of PMMA and AlN (above) with schematic representation of the coatings (below). Not to scale.

Evaluation of the NRL Polymer's refractive index provided a transmission model, seen in Figure 20, which was less than the targeted 99.5%. The model prescribed identical structures on the front and back surfaces consisting of 97 nm of the NRL polymer and an external 10 nm thick SiO_2.

Table 3. Model prescription for a NRLP based antireflective coating for polycarbonate.

Material	Thickness (nm)
Front	
NRLP	97
SiO_2	10
Back	
NRLP	97
SiO_2	10

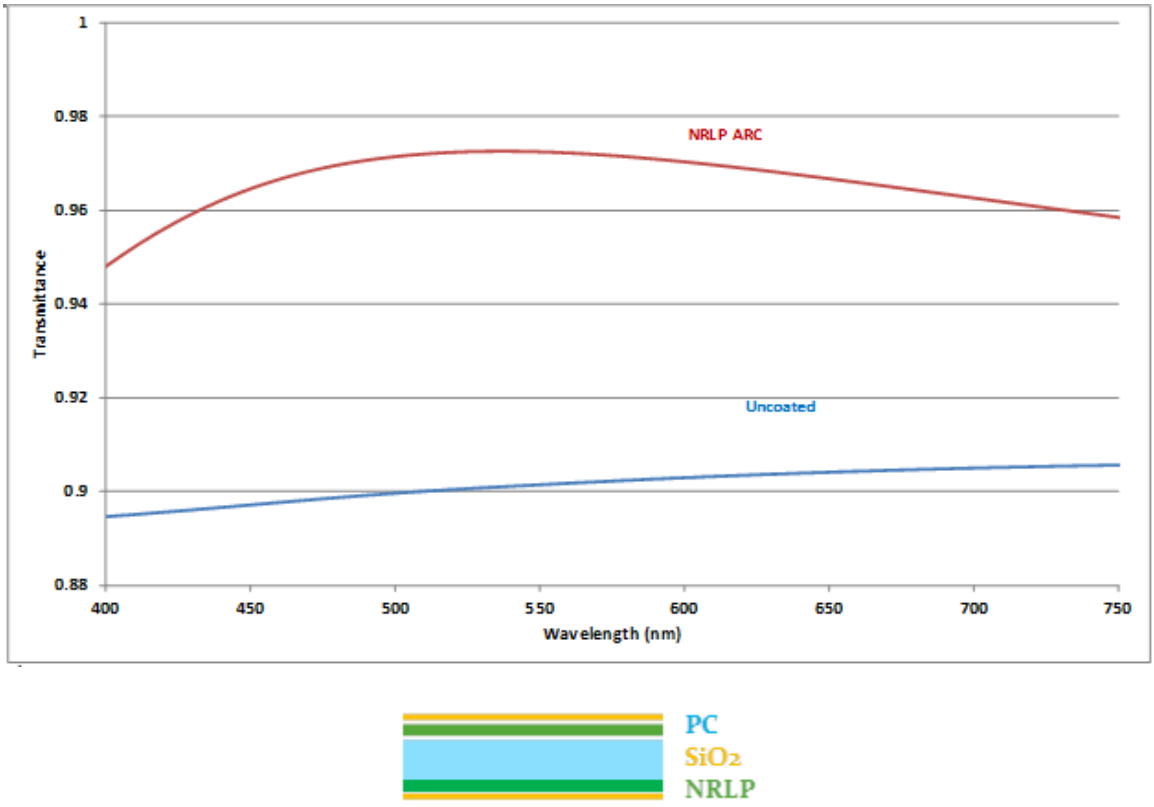

Figure 20. Model of the SiO_2/NRLP ARC for PC window (top) and the schematic representation of the coating (bottom).

MAPLE System and Process Development

MAPLE techniques vary depending on equipment used, particularly the type of laser. The laser used in this study is an Er:YAG laser (2937 nm, Big Sky Lasers) which emits in the infrared. Generally, all processes start with a laser light source focused on a solid matrix target consisting of a dilute frozen solution in thermal contact with a liquid nitrogen cooled base, seen in Figures 21 and 22. Once excited by the laser, the matrix solvent molecules selectively vaporize to form an energetic plume off of the surface of the target carrying with it any non-volatile molecules, such as polymers. To encourage homogenous vaporization and uniform deposition, the conditions at the target surface where the laser interacts with the matrix must be consistent with each pulse. Methods to achieve this include slow rotation of the target matrix, or rastering the incoming beam across a stationary target using a motorized programmable mirror in the beam path prior to entering the target chamber. These methods allow for a fresh frozen surface for each pulse. Other methods to encourage homogeneity will be discussed that focus on formation of the matrix. The MAPLE chamber is under vacuum so that volatile solvent molecules are removed prior to reaching the substrate. Solvent contamination of the deposited film is a concern for most MAPLE applications.[30] If necessary, post-deposition annealing can free residual solvent from the film and improve film quality.[23] Larger molecules which are not in a gas phase will ideally have enough velocity from the ejected plume to deposit on the substrate centered directly above the laser-matrix focal point at an experimentally determined distance.

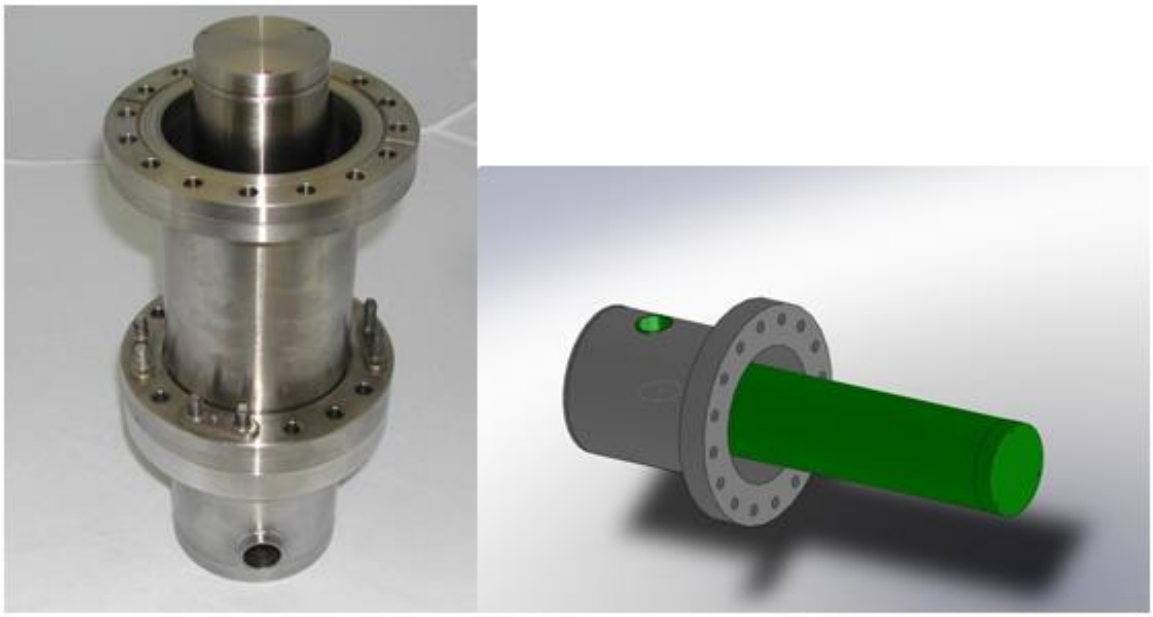

Figure 21. The liquid nitrogen cooled base developed for the MAPLE system. A schematic is shown on the left and the actual piece with an additional nipple is shown on the right. The cold face is 6.35 cm in diameter.

Figure 22. The MAPLE target holder. The disassembled structure (mount and target holder) is on the left and assembled structure is on the right. The two are held together by magnets.

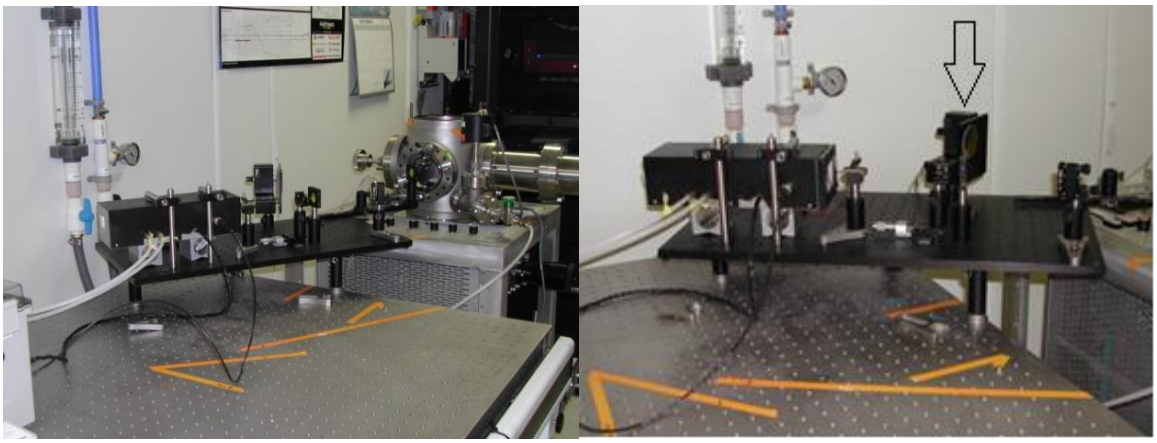

Figure 23. The MAPLE system developed for this project. The full system is shown on the left and a close-up of the optics on the right. The key component of the optics is the moving mirror (arrow) that allows rastering of the beam across the target.

The complete MAPLE system used in this work is shown in Figure 23. One key component of the optical system is a translating mirror system that will allow the laser beam to be rastered across the target surface. This programmable mirror allows effective use of the majority of the target ensuring a frozen surface with each pulse. The operating MAPLE system is shown in Figure 24 note the liquid nitrogen reservoir. The optical system ray trace is shown in Figure 25. The laser beam is focused using a series of CaF_2 optics into a turbo-pumped vacuum chamber with a base pressure ~1 x 10^{-6} Torr. The beam enters the chamber through a CaF_2 window. The spot size of the focused laser beam at the target was determined using thermal absorption paper (Zap-It) and was measured to be ~0.057 cm^2.

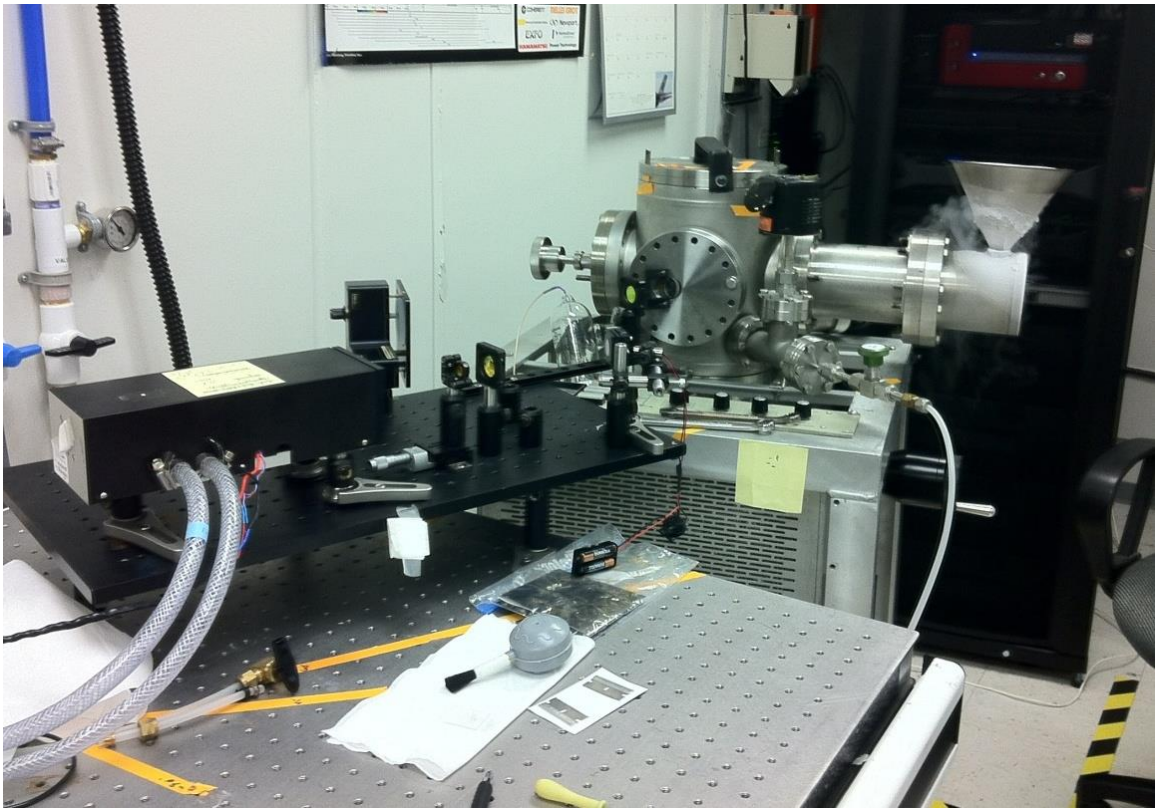

Figure 24. The RIR-MAPLE system. The system uses an Er:YAG laser and rasters the beam across the target using a motorized mirror.

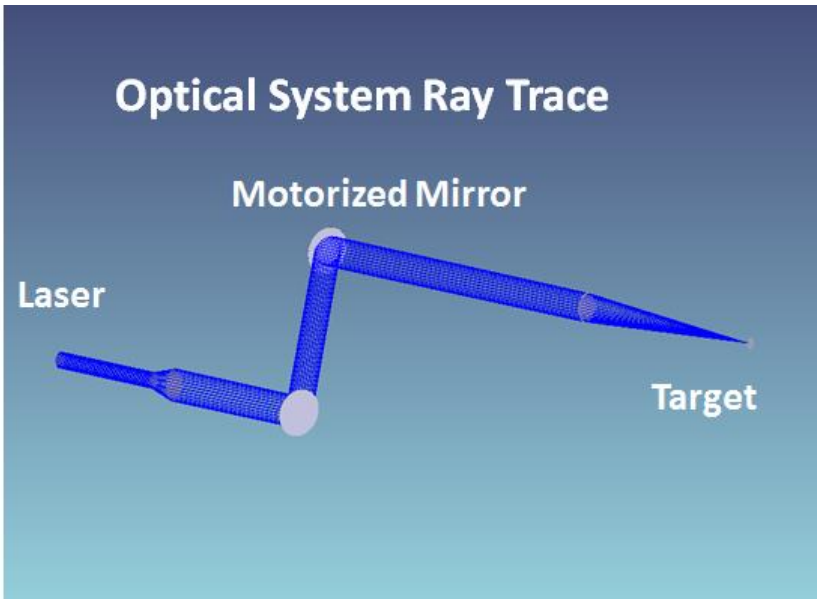

Figure 25. The optical system ray trace for the RIR-MAPLE system.

The process flow for MAPLE deposition is:

1) Fill the cold finger with liquid nitrogen until the cold finger stabilizes in temperature.
2) Fill a target holder with dilute polymer solution, and keep immersed in liquid nitrogen until the target is placed in the chamber.
3) Bring the vacuum system up to atmospheric pressure.
4) While continually flushing the vacuum system with dry nitrogen, open the chamber and mount the target.
5) Mount the sample(s) on the sample mount.
6) Close and evacuate the chamber.
7) Bring the system to the deposition pressure by leaking in nitrogen through a leak valve. The deposition pressure is approximately 10 mTorr.
8) Fire the laser at the target for the desired number of pulses.
9) Pressurize the chamber and remove the samples and target, if necessary, after the deposition.

Interaction between laser and matrix is the mechanism which affects thin film properties. Laser settings and optical setup vary widely between MAPLE techniques. Laser variables such as power output, spot size, fluence, pulse frequency, and pulse duration are adjustable. Typically, though not always, a laser will have a specific set wavelength. The deposition process is dependent on the matrix's ability to absorb the emitted wavelength sufficiently so to vaporize the frozen solvent. Some MAPLE processes use lasers that emit in the ultraviolet. Many solvents absorb ultraviolet light enough for a functional deposition event. A significant drawback for an ultraviolet

MAPLE process is the potential degradation of any non-solvent molecules by the ultraviolet light due to the near ubiquitous absorbance from all molecules in the matrix. Alternatively, infrared lasers are very effective for MAPLE applications since the wavelength matches nicely with the absorbance seen by matrix solvent functional groups such as alcohols and amines. This specificity is the primary benefit of RIR-MAPLE over more traditional UV MAPLE processes.

MAPLE experimental design depends on two parameters, laser wavelength and matrix composition. Components of the matrix to consider are the desired deposition molecules, a primary solvent to get those molecules into solution, and if needed, other solvent components designed to solvate polar side chains to open up polymer molecules or to facilitate in absorption of the irradiating light. The primary solvent must be able to keep the polymer dispersed in solution as well as in the frozen matrix. Congregation and partial dissolution of polymers while freezing are detrimental to MAPLE processes. Matrix homogeneity will directly affect film quality.[29] Large congregates in the matrix will result in large defects in the film.[29] Secondary solvents can help open up and spread out polymers in solution. If a secondary solvent is used, phase segregation of the solvents is a potential concern while freezing the matrix. In some cases, solubility testing is necessary to determine appropriate ratios.

Targets were prepared by partially submerging a target holder just into a liquid nitrogen (LN2) bath and then slowly filling the puck with the sample solution. Targets were allowed to slowly freeze in a continuous manner from the surfaces of the holder inward. Freezing samples were watched carefully for any phase separation that could cause the targets to form inappropriately. Phase segregated samples were not used. A

freezing target can be seen in Figure 26. After samples had sufficiently frozen, they were immersed in the LN2 and hardened for several seconds. The target was then ready for placement in the MAPLE chamber.

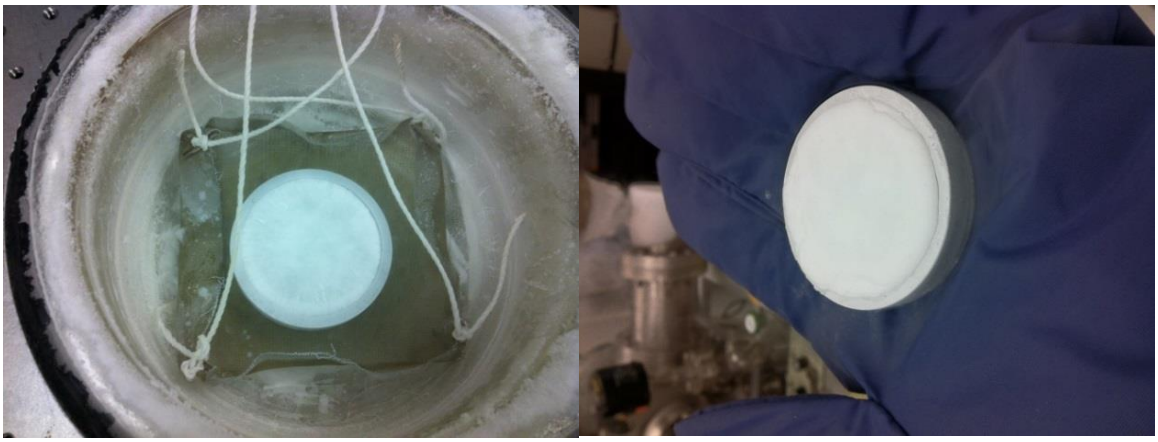

Figure 26. A target being prepared (left) and the finished target (right).

Phase segregation is detrimental to an ideal MAPLE matrix. The ideal matrix will be opaque and homogeneous. This scenario can be seen in Figure 7, specifically the rightmost image. The physical basis for this being that the ideal matrix configuration is one that prevents penetration of the laser beam farther than can be maximally absorbed. Energetically, this maximizes the amount of energy absorbed per unit volume of the matrix. Absorption of energy is the primary function of the matrix and allows the energetic plume to be as effective as possible to eject the solutes. The other extreme is the image on the left. This matrix was formed using a ternary solvent, tetrahydrofuran (THF), as an intermediate between methanol and toluene. This frozen matrix seems homogenous, which was the goal of the new solution; however the transparency of the matrix prevented maximal absorbance of the laser which allowed the light to reach the base of the target holder. The matrix immediately melted under laser excitation. This

matrix only survived the MAPLE process for a matter of seconds despite being at an appropriate temperature and in contact with the liquid nitrogen cold finger base. The limited thermal tolerance of this matrix is not necessarily due to the arrangement of the frozen molecules, but with the interaction the matrix has with the laser. The laser is allowed to penetrate through the transparent matrix significantly farther than in the ideal matrix. The consequence of this is dramatically reduced energy density absorption resulting in minimal excitation of the hydroxyl bonds which effectively melts a large volume instead of vaporizing a small one. The intermediate image in Figure 7 is representative of the previously mentioned phase segregation. The opaque areas are likely toluene which froze ahead of the rest of the solution. Careful attention must be given to ensure proper matrix formation. Once produced, an ideal matrix can be healed with its original solution, maintaining the preferred appearance over multiple depositions.

Initial matrix design for this study was based on Hansen Solubility Parameters,[28] for a Polymethylmethacrylate (PMMA) solution with both toluene and methanol.[29] Toluene alone is an effective solvent for PMMA, but has insufficient absorbance of the IR wavelength (2937 nm) emitted by the Er:YAG laser. The methanol in the solution provides two desirable attributes. First, the methanol helps to spread out the polar acrylic pendant groups that would otherwise tend to cluster in solution with toluene alone, forcing the polymer chains into a compact droplet configuration in solution and in the matrix which would result in increased roughness of the film.[27] Second, the bond between oxygen and hydrogen of the methanol significantly absorbs a broad range in the infrared spectrum between 3200-3600 wavenumbers (cm^{-1}). The corresponding value for the laser's wavelength of 2937 nm is approximately 3405 cm^{-1} making the small alcohol

a crucial component of the matrix providing essential dispersion and absorption for the MAPLE mechanism.

To relate film quality to the primary solvent, a study of three solvents was conducted. The solvents investigated were benzene (EMD, DriSolv), toluene (EM, GC grade), and p-xylene (Capitol, reagent grade) for use with PMMA (Aldrich, avg. MW ~120k). These solvents all readily dissolve PMMA, are non-corrosive, and have relatively high freezing points. High freezing points enable the targets to more easily remain frozen when attached to the cold finger in the MAPLE system while under laser excitation. The problem with using these three solvents is that they do not absorb at the laser's wavelength, 2937 nm. That problem is easily overcome by addition of methanol (Pharmco-Aaper, reagent grade) as previously discussed.

While freezing the solutions, solubility limits may be reached as the temperature drops. Maximizing solubility can prove necessary to produce adequate films. As mentioned in the previous paragraph, the initial matrix solution was based off of Hansen solubility parameters.[28] Hansen found that the amount of a polymer that could be placed into a solvent was a function of the dispersion forces (δ_d), polarity (δ_p), and hydrogen bonding (δ_h) of both the polymer and the solvent.[28] In the case of multiple solvents, the molar average of values can be used. The solubility radius (R_a) of the polymer in parameter space is then defined as:

$$R_a = [4(\delta_{d1} - \delta_{d2})^2 + (\delta_{p1} - \delta_{p2})^2 + (\delta_{h1} - \delta_{h2})^2]^{0.5}$$

The subscript 1 refers to the solvent and subscript 2 refers to the polymer. R_a can be used to define a sphere with constraints $2\delta_d$, δ_p, and δ_h. If the Hansen solubility parameters for the solvent fall within the polymer "sphere" in parameter space, the solvent is very likely

to solvate the polymer. For components of this investigation, the Hansen parameters are given in Table 4.

Table 4. Hansen solubility parameters

	δ_d (MPa$^{0.5}$)	δ_p (MPa$^{0.5}$)	δ_h (MPa$^{0.5}$)	R_o (MPa$^{0.5}$)
Benzene	18.4	0	2.0	---
Toluene	18	1.43	2.05	---
Xylene	17.8	1.0	3.1	---
Methanol	15.1	12.3	22.3	---
PMMA	18.6	10.5	7.5	8.6

This data provides an ideal solvent combination for a given polymer solution. In the case of the toluene, methanol, PMMA system, it resulted in an 84 weight percent toluene and 16 weight percent methanol solution, shown in Figure 6.[29] This solution was used as a starting point for the Designed experimental solutions which normalized the methanol weight percentages. FTIR spectra (Nicolet iS10, 4 cm^{-1} resolution, 16 scans averaged, samples placed in a ZnSe cell) of the solutions are shown in the following Figures (27-29). The –OH band due to the addition of methanol is easily seen from 3300-3500 cm^{-1}. The wavelength of the Er:YAG laser is displayed at 3405 cm^{-1}.

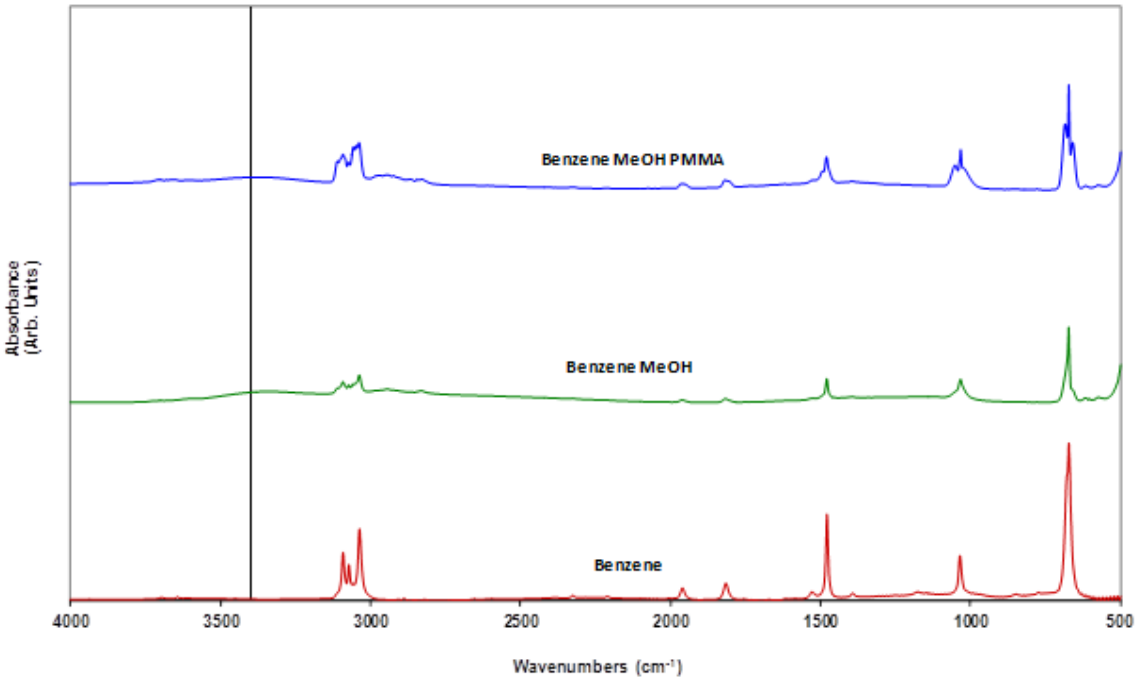

Figure 27. FTIR spectra of Benzene solutions. The vertical line represents the laser wavelength.

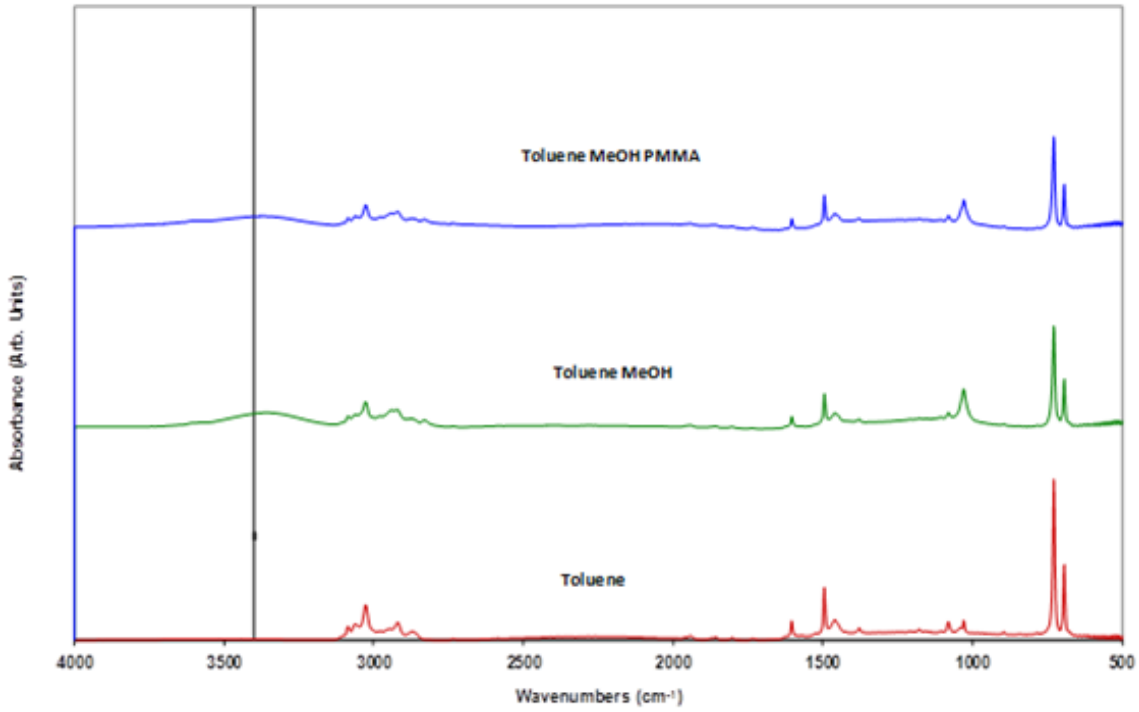

Figure 28. FTIR spectra of Toluene solutions.

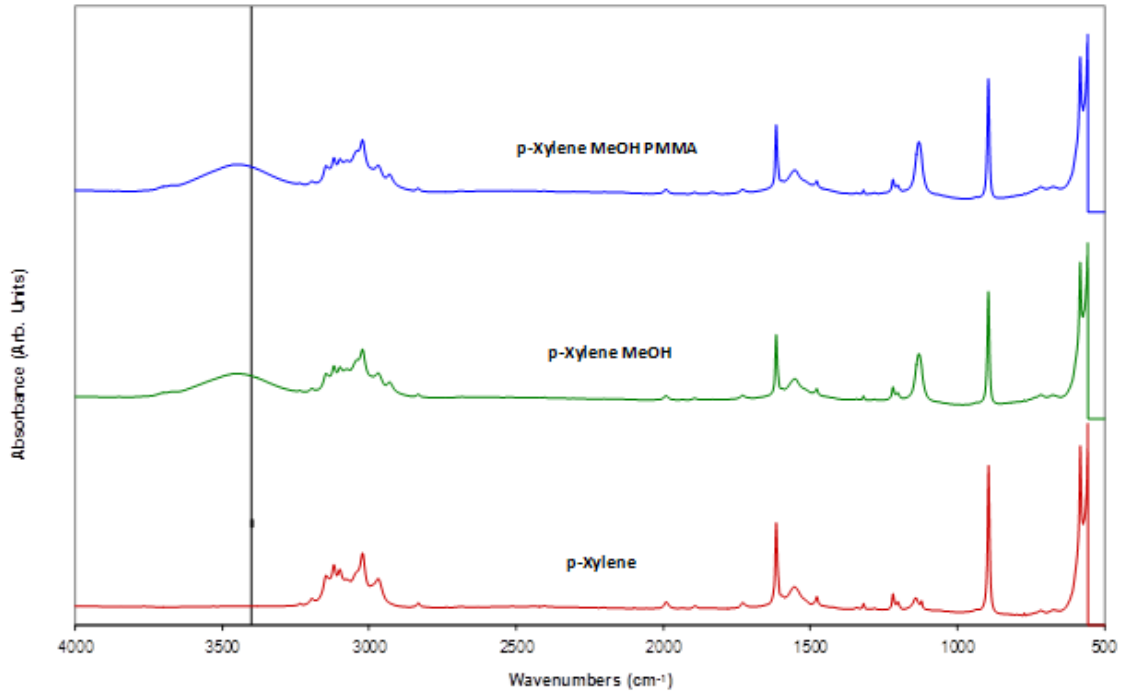

Figure 29. FTIR spectra of p-Xylene solutions.

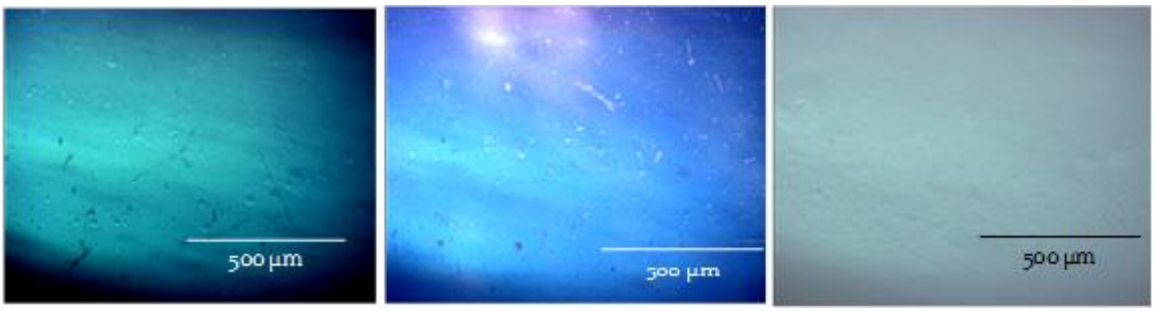

Figure 30. Optical microscope photos of thin PMMA films prepared using MAPLE and various target solutions. The film on the left was produced using a 1 wt% PMMA in 84:16 benzene:methanol. The central film was produced with the same concentrations in a p-xylene based solution. The toluene solution on the right can be seen to have the lowest number of large defects.

Figure 30 shows representative films from the three solvent study. JMP 5.0 experimental design software was used to optimize process parameters for optical quality coatings. Experimental variables were: solvent, polymer concentration, laser fluence, and

distance of the substrate from the target. Responses obtained included: film thickness, uniformity, surface roughness, and defect density. The 1 wt% solutions shown in Figure 30 were the upper concentration limit of the experiment. Toluene consistently produced the highest quality films with the lowest defect density and roughness. Results are displayed in Figure 31.

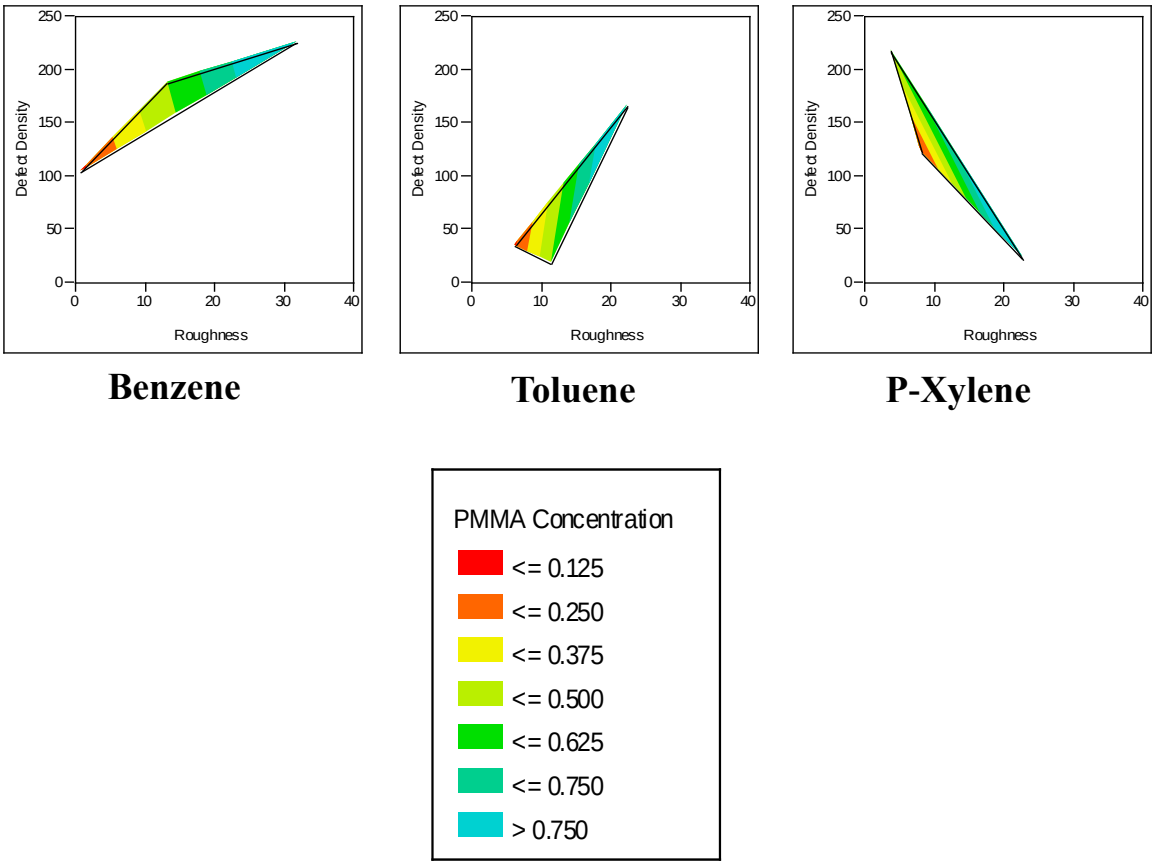

Figure 31. DOE of the three solvents comparing concentration effects on roughness and defect density.

PMMA

Recall that the PMMA-based ARC model used a repeating set of sputter deposited SiO_2 and MAPLE deposited PMMA (see Table 2). The initial layers of SiO_2 were reactively sputter deposited using the magnetron sputtering system described in the last

report. Specifically, a Si target (Lesker, 99.999%) was sputtered in a mixture of 50:50 Ar:O_2 at 200 W and 5 mTorr. The polycarbonate window was held at 25 °C throughout the deposition. Film thickness was measured using interferometry (Filmetrics F20) and, in some cases, profilometry (Dektak 150). The PMMA layers were deposited using MAPLE (2937 nm, 350 μsec pulse, fluence = 5.25 J/cm^2) and a target of 0.05% PMMA (Aldrich) in 84 wt% toluene / 16 wt% methanol. The deposition pressure was 10 mTorr. Using predetermined deposition parameters, proper film thicknesses could easily be achieved.

NRLP

The NRLP-based ARC uses a combination of NRLP and SiO_2, as was previously described in Table 3. In this case, the NRLP was initially MAPLE deposited (2937 nm, 350 μsec pulse, power = 500 mW, fluence = 0.88 J/cm^2) onto a cleaned PC blank using a target of 0.05% NRLP (ExFluor) in 95 wt% methanol / 5 wt% methyl ethyl ketone. The deposition pressure was 10 mTorr. Using predetermined deposition rates, the proper film thicknesses were again easily achieved. The SiO_2 was deposited using magnetron sputtering, as previously described. A FTIR spectrum of the NRLP in MEK is seen in Figure 32. The polymer has some absorption at the IR laser wavelength. This problem is alleviated by the very low polymer concentration coupled with the dramatically increased concentration of methanol in this matrix solution, 0.05% compared to 95% by weight. The hydroxyl contribution to the weight of the methanol is also similarly increased compared to the heavy fluorine containing polymer.

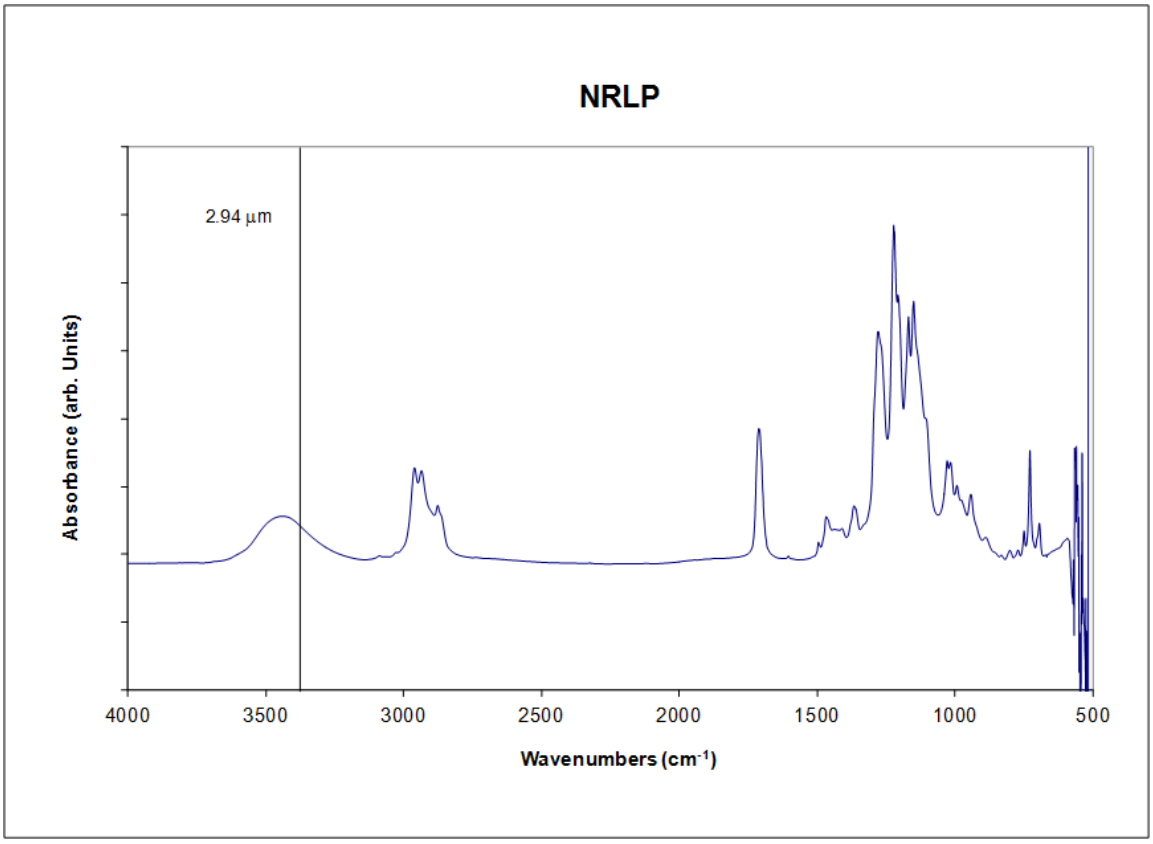

Figure 32. FTIR spectra of NRLP (70% by weight solution in MAK). The absorbance at the Er:YAG laser line is again shown.

Teflon® AF

It was found that Teflon® AF (TAF) solubility was limited to one solvent, Fluorinert™ (DuPont™ FC-40; a fully fluorinated mixture of $C_5 – C_{18}$ compounds). There are no Hansen parameters for this solution. As the solvated TAF has no absorption at 2937 nm, a solvent that is miscible with Fluorinert™ and has an –OH functional group had to be added. Two such solvents were evaluated: perfluoro-t-butanol (Oakwood Chemical) and 1H, 1H-perfluorohexanol (PFH, ExFluor). Due to the cost and reported toxicity of the perfluoro-t-butanol, we concentrated on the PFH. FTIR spectra of TAF solutions containing various PFH concentrations can be seen in Figure 33.

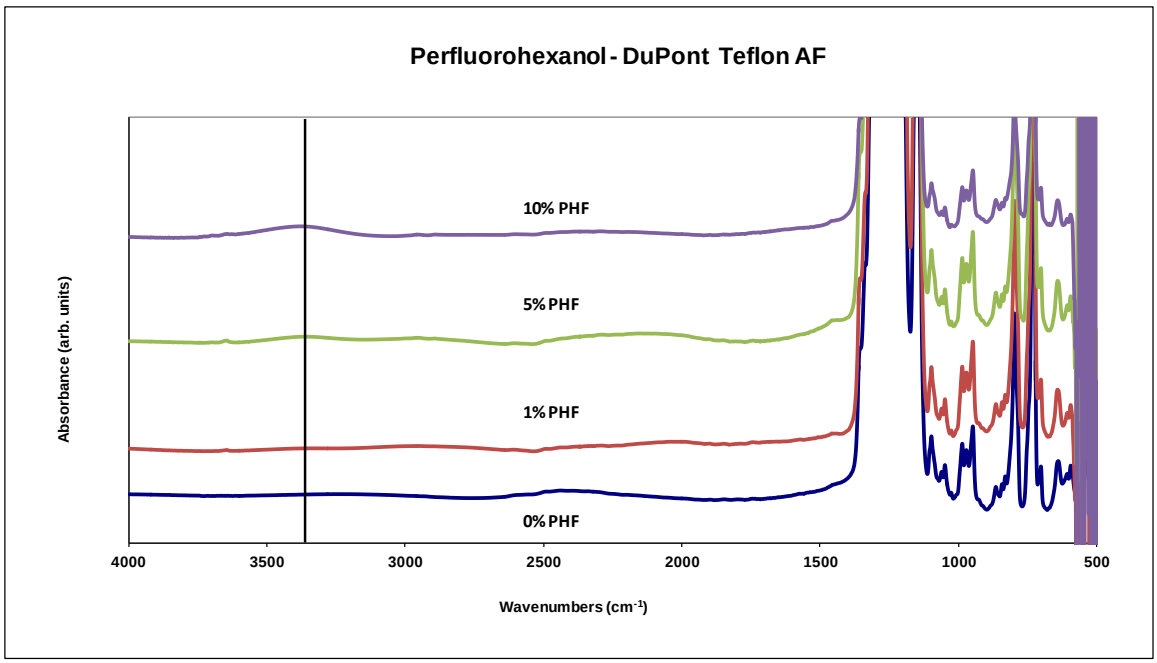

Figure 33. FTIR spectra of DuPont™ Teflon® AF (1% by weight solution in Fluorinert™) and various concentrations of 1H, 1H-perfluorohexanol (PFH). Note the absorbance at the Er:YAG laser line for the more concentrated solutions.

CHAPTER 4

RESULTS AND DISCUSSION

PMMA

While polycarbonate flats were the eventual substrate intended for deposition, glass slides were used initially to develop the deposition process and fine tune parameters. Designed experiments were set in place to investigate the effect of each proposed parameter on the deposition rate and film quality. The first designed experiment (DOE) was set to determine the best solvent system for a polymethylmethacrylate (PMMA) solution. Literature sources indicated that a solution of methanol and toluene would be a valid basis for this investigation.[29] As previously mentioned, the aromatic family of toluene, benzene, and p-xylene was investigated. The literature source prescribed a methanol to toluene weight ratio of 16:84, based off of Hansen Solubility Parameters, to maximize the solubility of PMMA. This methanol weight ratio was held constant across the DOE. The results of the DOE as formed by the JMP 5.0 DOE software are seen in Figure 31. Toluene, in agreement with the literature source, was the optimal solution for minimization of roughness and defect density. Consistent with each solvent system is the superiority of a dilute polymer solution for increasing film quality, this correlation is discussed later. Film thickness and roughness measurements were carried out using a Filmetrics F20. Defect density was manually counted per a set surface area on an optical microscope. The PMMA coatings produced

by MAPLE deposition on glass substrates were used to develop the deposition process, both initially and corresponding to the DOE are listed in Table 5.

Table 5. MAPLE produced PMMA coatings on glass substrates.

PMMA (weight %)	Solvent to Methanol Ratio	Pulses	Thickness (nm)	Roughness (nm)	Uniformity (%)
1	Benzene 90:10	Range	83.73	17.79	80
1	Benzene 90:10	750	54.04	12.45	70
1	Benzene 90:10	810	31.36	10.54	69
1	Benzene 90:10	1110	28.43	13.16	83
1	Benzene 90:10	1290	15.83	13.4	11
0.5	Toluene 84:16	2000	35.68	11.98	66
0.5	Toluene 84:16	3000	57.01	14.92	83
1	P-Xylene 84:16	3000	54.38	9.01	89
1	P-Xylene 84:16	1500	53.07	6.43	77
1	Benzene 84:16	3000	60.23	6.74	87
1	Toluene 84:16	3000	72.87	14.44	88
1	Toluene 84:16	1500	64.69	11.22	92
0.5	Benzene 84:16	3000	83.14	13.37	87
0.1	Toluene 84:16	3000	53.28	6.27	78
0.1	P-Xylene 84:16	3000	65.84	8.34	96
0.1	Benzene 84:16	3000	5.33	0.89	81
0.5	P-Xylene 84:16	3000	69.23	3.97	90
1	P-Xylene 84:16	3000	122.24	15.05	86
1	Benzene 84:16	3000	128.74	31.93	87
1	Toluene 84:16	3000	77.15	17.01	55
1	Toluene 84:16	3000	90.47	22.93	88
1	Toluene 84:16	3000	94.5	22.5	90
0.5	Toluene 84:16	3000	80.39	11.6	87
0.5	Toluene 84:16	3000	52.86	16.5	39
0.5	Toluene 84:16	3000	65.9	15.6	54
0.5	Toluene 84:16	6000	67.8	23.4	76
0.5	Toluene 84:16	3680	71.01	17.96	66
0.1	Toluene 84:16	9000	36.9	11.2	54
0.1	Toluene 84:16	12000	45.6	14.2	82
0.1	Toluene 84:16	3000	41.62	---	87
0.1	Toluene 84:16	6000	41.19	---	92
0.1	Toluene 84:16	9000	47.92	---	94
1	Toluene 84:16	3000	57.92	---	89
1	Toluene 84:16	6000	60.1	---	92
1	Toluene 84:16	9000	57.79	---	---

The toluene solution was used to fine tune the deposition parameters. Blank data points in Table 5 are a result of instrument availability. Once deposition methods were established, ARCs were produced on PC substrates. An AR coated PC window is shown in Figure 34. The transmission and front surface reflectance spectra are shown in Figures 35 and 36. Recall that the modeled transmission for this coating is >98% from 400-750 nm. The best MAPLE produced PMMA ARCs only showed modest improvement over an untreated PC sample. Finished film thicknesses had been measured and were found to be correct according to the modeled ARC. It is believed that the MAPLE depositions were still too rough to provide the desired transmission. As stated previously, the roughness of the MAPLE deposited films is the primary hurdle for optical applications.

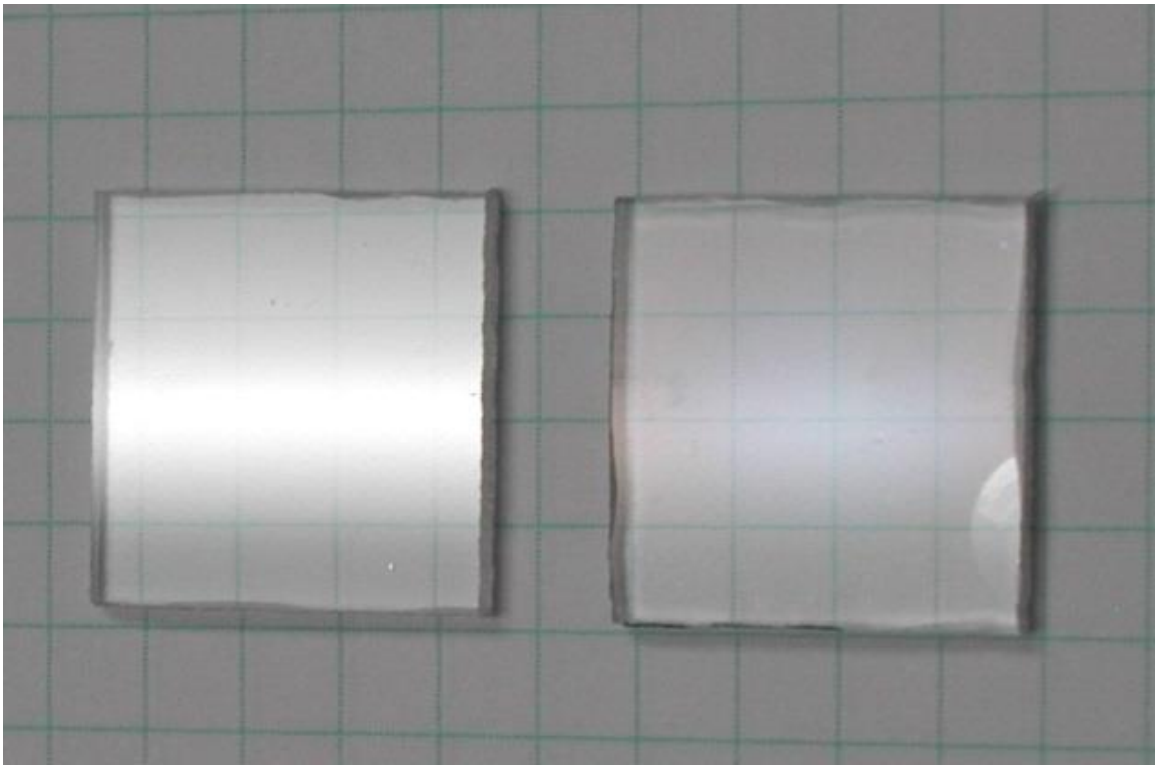

Figure 34. Comparison of a blank PC substrate (left) and a PMMA-based ARC (right). The ARC was produced according to the prescribed model in Table 2. The reflection of the overhead fluorescent light is significantly reduced.

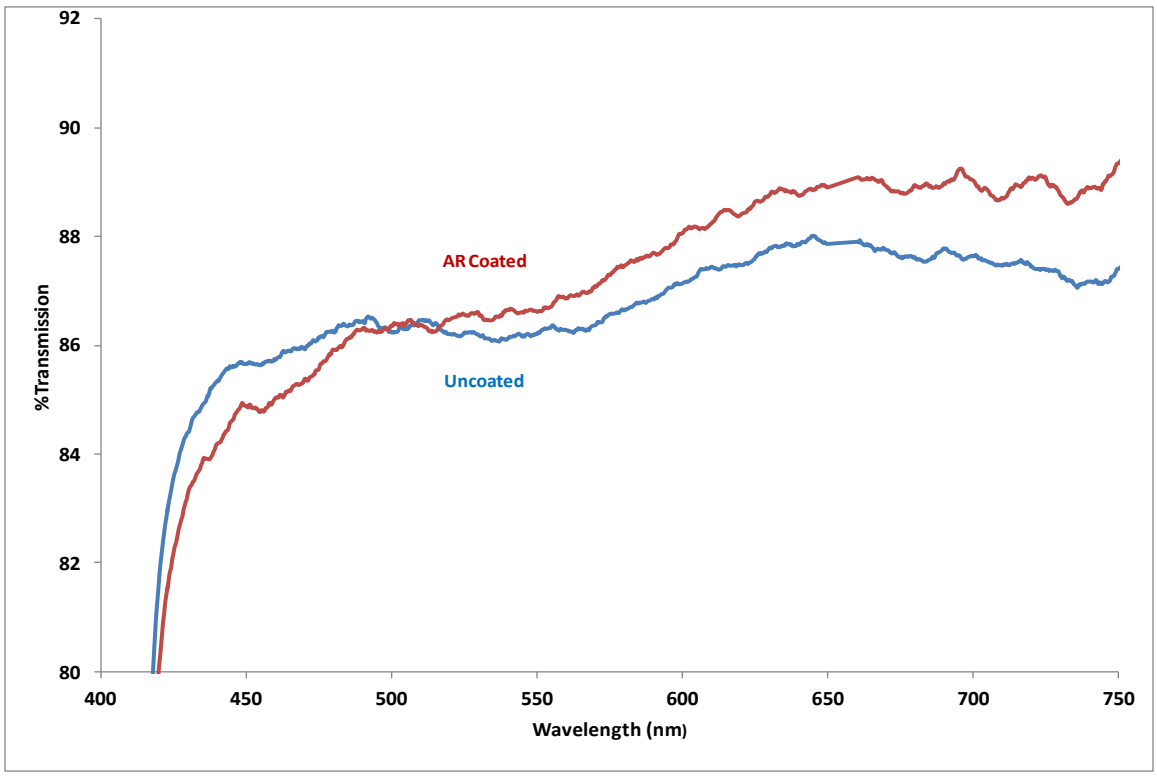

Figure 35. Transmission of the PMMA coated MAPLE produced ARC on PC substrate.

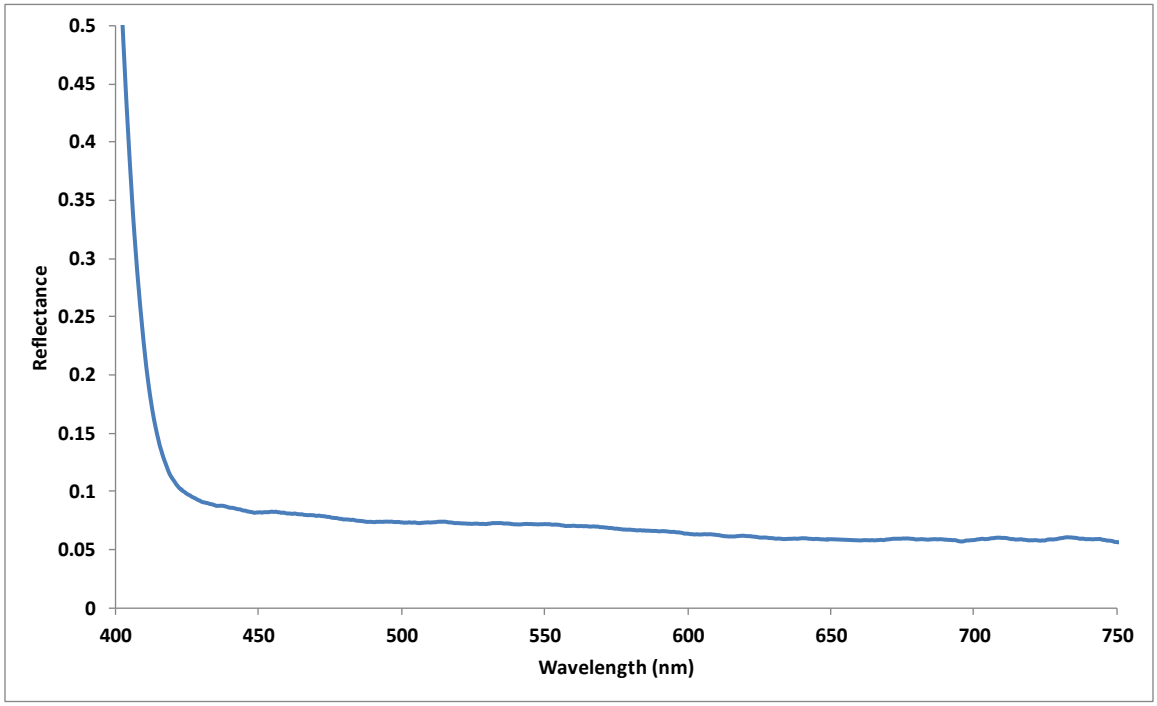

Figure 36. Front surface reflectance of the MAPLE deposited PMMA-based ARC on PC substrate.

As is apparent in Figure 34 and can be verified in Figure 36, the MAPLE produced PMMA ARCs were significantly antireflective. However as can be seen in Figure 35 the transmission of the total structure falls well short of target goals. In addition to the roughness of the film creating scattering which limits transmission, the PC flats used in this work had significant absorption which further decreased transmission. Additional MAPLE matrix solutions are discussed below.

Teflon® AF

To verify the model described in the materials and methods chapter, the prescribed stack was coated onto an untreated polycarbonate flat (SABIC, 3 mm thick) using magnetron sputtering for the SiO_2 layer and spin coating for the Teflon® AF (DuPont™; 1% Teflon® AF in Fluorinert™) coating. The spin coating was done using a Laurell Technologies spin coater (Model no. WS-400B-6NPP/LITE) after spin-speed curves were obtained to achieve the proper thickness deposition parameters. A photo of the coated piece is shown in Figure 37. The transmission spectrum of the coated polycarbonate window is shown in Figure 38, and the front surface reflection in Figure 39. The transmission of the coated window is below the desired 99.5% transmission due largely to inherent absorbance of the PC. Reflectance was found to be under 0.5% for most of the visible spectrum. The reduction in reflection is readily apparent.

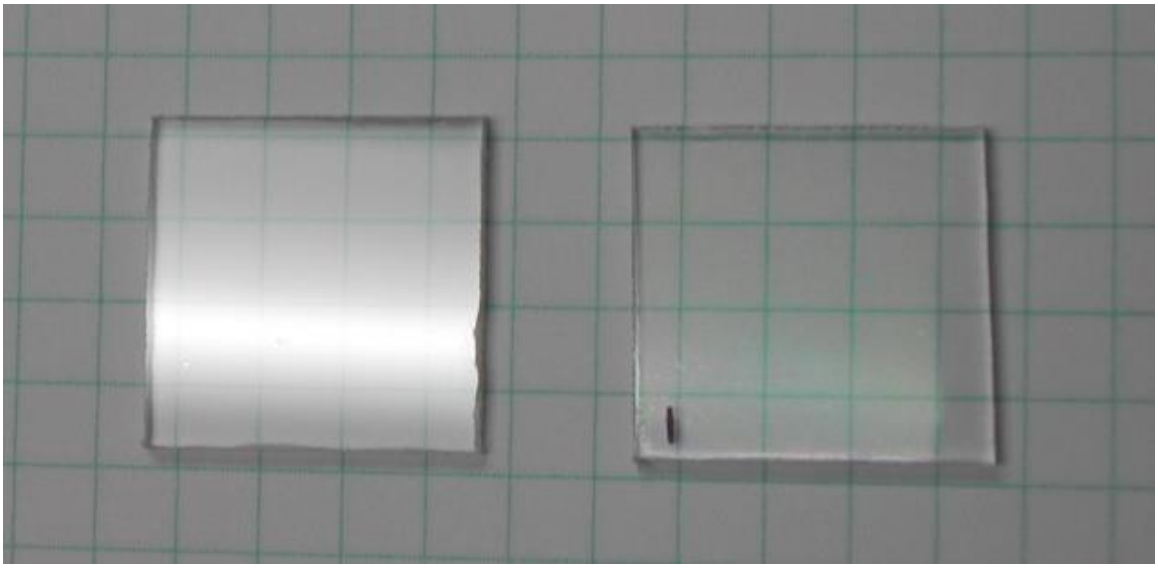

Figure 37. Photo of an uncoated PC window (left) and an AR coated PC window (right). The reflection of an overhead fluorescent light is greatly reduced.

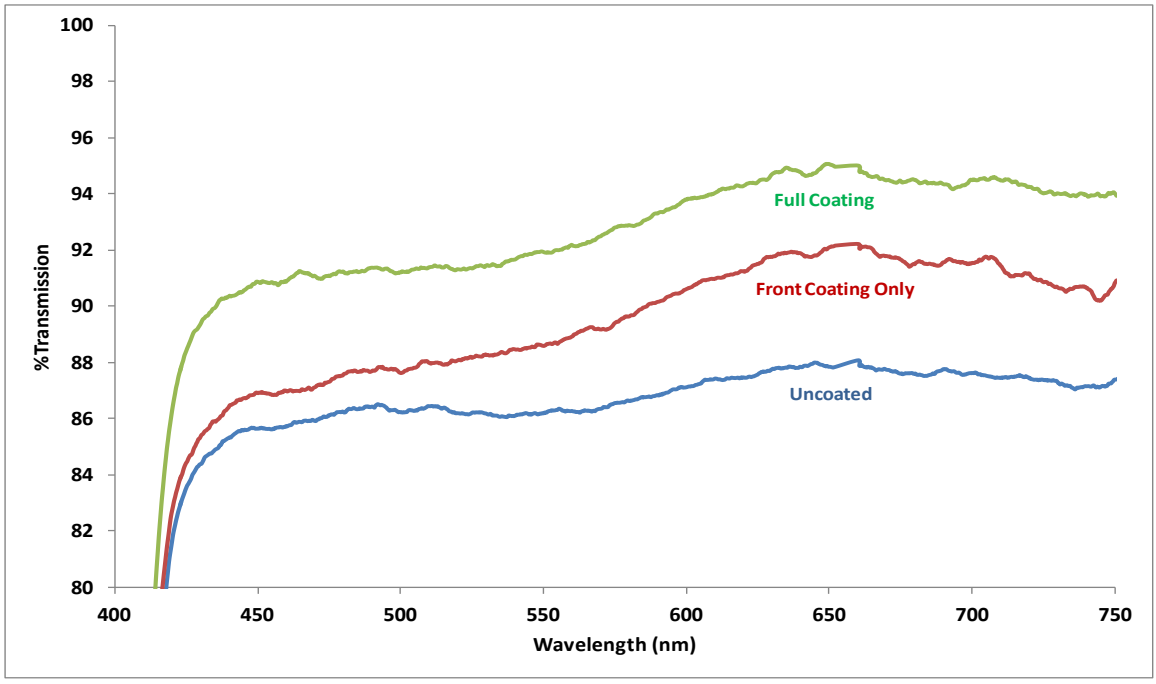

Figure 38. Transmission spectra of the SiO_2/Teflon® AF AR coated PC window.

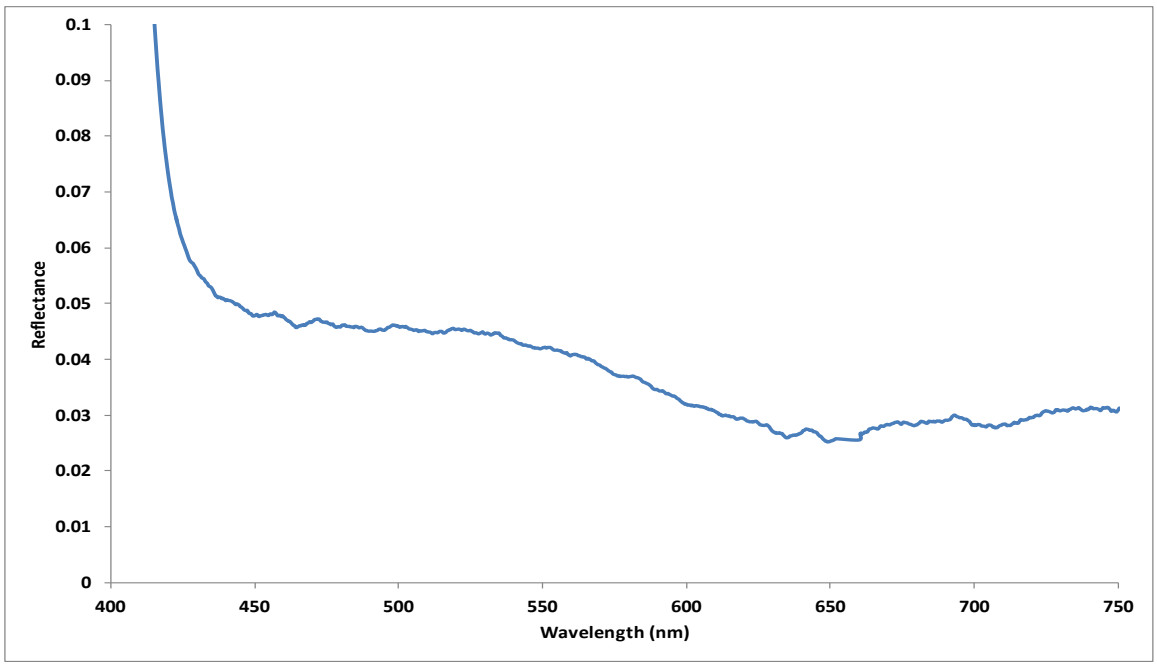

Figure 39. Reflectance spectrum for the SiO_2/Teflon® AF AR coated PC windows.

Teflon® AF MAPLE depositions were not promising, as shown in Figure 40. Optical microscopy shows layers of fibrous strands with no continuous film. The strand count increased with the concentration of perfluorohexanol (PFH). This is due to the increased hydroxyl group content in the matrix and the resulting increased absorbance of irradiating light facilitating the deposition mechanism. Through solubility testing it was evident that despite PFH and Fluorinert™ being infinitely miscible, the 1% of TAF in the Fluorinert™ precipitated out of solution with weight percentages of PFH as low as 15%. This concentration of hydroxyl groups would be insufficient for MAPLE deposition. Recall that the PMMA solutions had a sixteen weight percent which, in comparison, is a significantly more effective solution due to the hydroxyl group contribution to the weight of methanol relative to the heavier fluorinated alcohol, PFH.

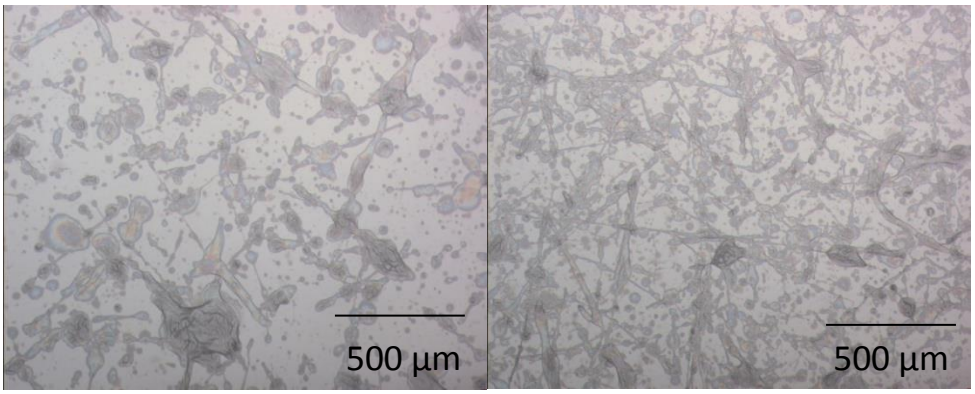

Figure 40. MAPLE depositions of 1% Teflon® AF in Fluorinert™ combined with various amounts of 1H, 1H-perfluorohexanol.

The failure of Teflon® AF to be successfully deposited using MAPLE is due to its limited solubility. While the properties and performance of the spin coated TAF ARC are discussed in the materials and methods chapter are very good, it is not compatible in solution with the high concentration of hydroxyl groups necessary for the MAPLE deposition mechanism. The solution to this problem would be to increase polar functional groups and potentially decrease the fluorine content of the polymer. This caused the NRL polymer to look more attractive. This polymer is not fully fluorinated and has oxygen containing functional groups available to increase solubility in alcohols. The structure can be reviewed in Figure 13.

NRLP

The NRL Polymer, NRLP, has superior solubility options compared to TAF. The importance of a high hydroxyl concentration for a MAPLE solution cannot be over stated. The presence of hydroxyl groups in the polymer itself only increases the need for

a high solvent hydroxyl concentration. NRLP comes as a 70% by weight solution in methyl amyl ketone. The stock solution was diluted with methyl ethyl ketone. The functional MAPLE solution of 5% diluted stock solution and 95% methanol which contained approximately 0.05% NRLP by weight. This concentration of the polymer in solution was low enough to allow for proper dispersion without being concerned with dissolution during matrix formation. The increased hydroxyl group concentration in the matrices containing the NRL polymer served two additional functions. First, the existence of hydroxyl groups in the polymer itself was a concern, as is visible in the FTIR data for the polymer Figure 32, the increased solvent concentration served to protect the polymer from degrading. Second, in order to decrease the roughness of the film, the energy density absorbed per unit matrix volume must be maximized[11]. Results from a designed experiment whose focus was to decrease roughness of the NRLP films as a function of polymer concentration and laser fluence are seen in Figure 41. The results indicate that the best films were obtained at the lowest studied polymer concentrations and laser fluences.

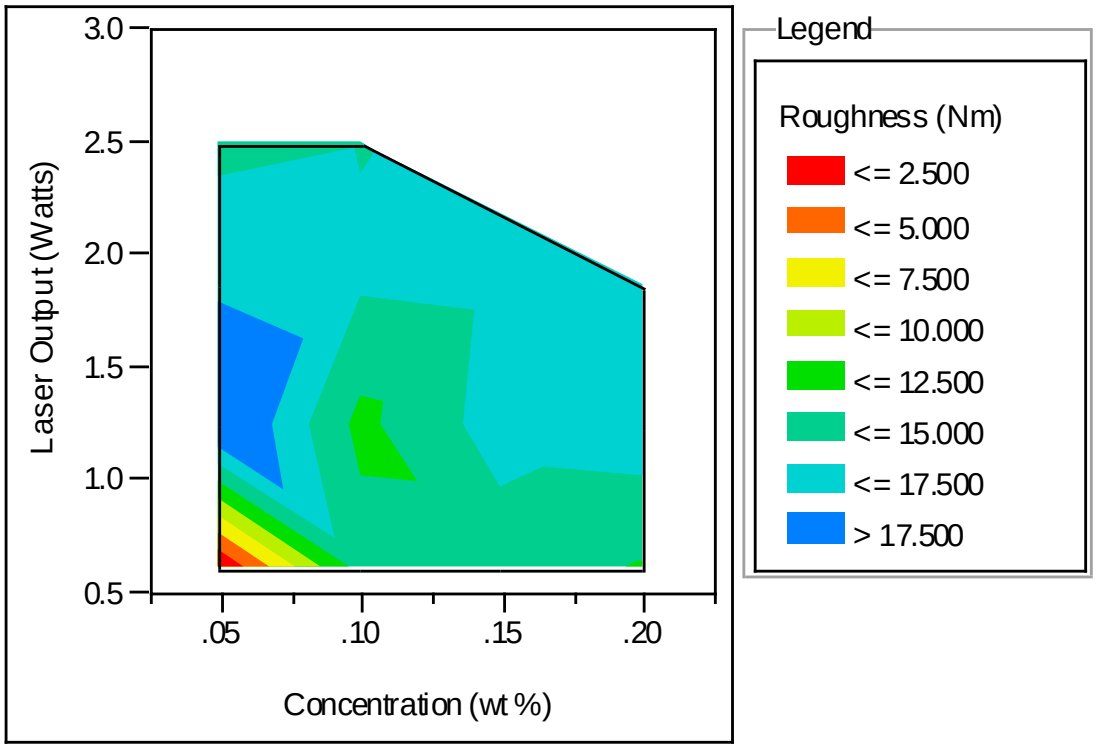

Figure 41. Contour plot for the NRLP films as a function of concentration and laser power. The best films in terms of film roughness were found to be at the lowest concentrations and laser fluences.

Despite the positive results from the lower concentrated matrix solutions, the modeled transmission data was again not reached by the finished product. Roughness of the film and absorbance by the PC flat persisted to limit transmission. Post deposition efforts to decrease light scattering by the film was a viable option. To investigate reflowing, or annealing, the films, thermal decomposition data needed to be obtained as it was not previously available for the NRLP. A thermogravimetric analysis (TGA, Universal V4.7A TA) was performed prior to annealing to ensure thermal stability limits would not be reached. The TGA can be seen in Figure 42. The weight percent versus temperature curve confirms the reported weight percent of the initial concentrated stock solution of 70 percent NRLP. MAK evaporates prior to decomposition of the polymer

which begins between 225-250° C. Based on this data, samples were annealed under vacuum at 200 °C and 100 mTorr for 24 hours.

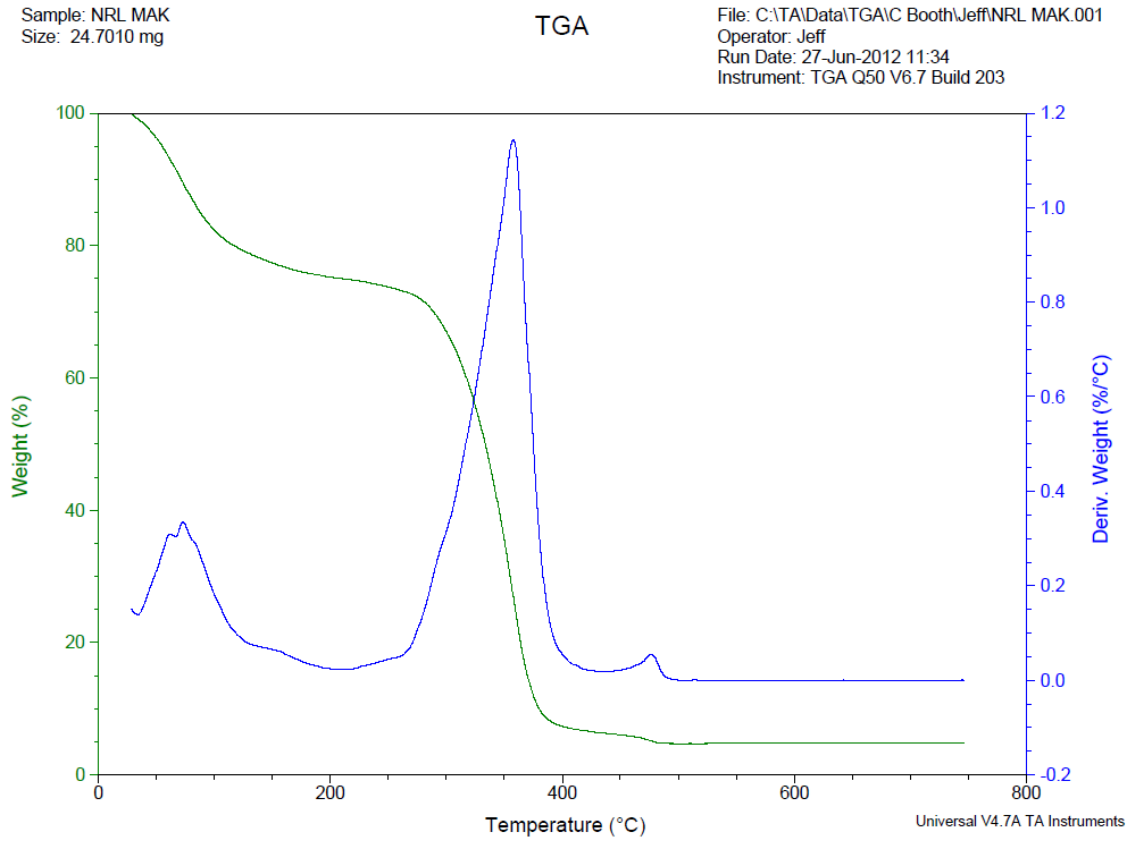

Figure 42. TGA of NRLP. The initial decomposition at ~75 °C is due to the evolution of the MAK solvent. The NRLP begins to decompose at ~225 °C.

Optical microscope photos of the as-deposited 0.05 wt% NRLP film using the 1:19 MEK:MeOH solvent matrix and reflowed films are shown in Figure 43. The impact of the annealing process is difficult to appreciate with this size of image; however the key difference between the two is the bubbles or mounds that are present in the as deposited sample and absent in the annealed sample. This improvement is more clearly appreciated in atomic force microscope scans (Nanoscope IV). In the scans in Figure 44, smoothing of the annealed film is apparent.

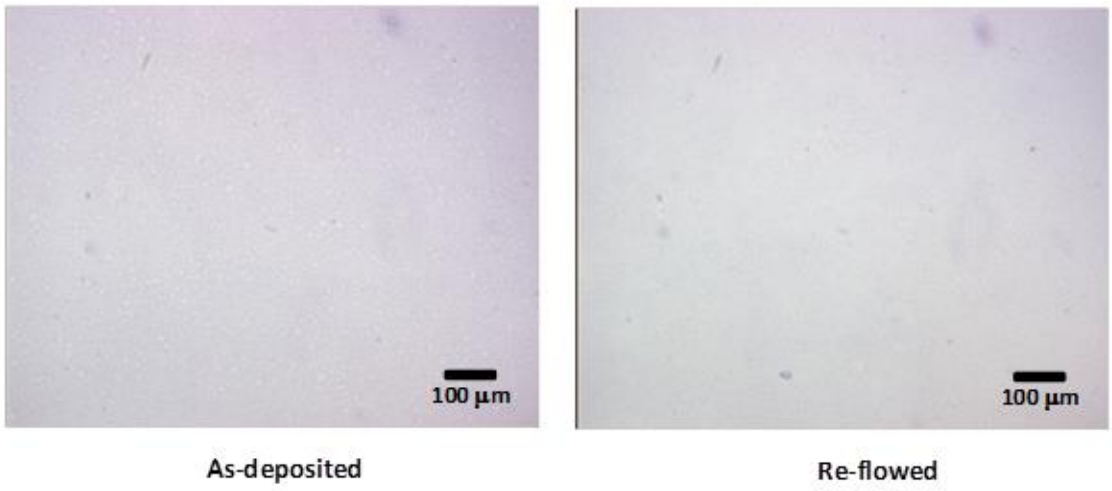

Figure 43. Optical micrographs showing effect of annealing. An as-deposited NRLP film is on the left, and a sample which was annealed at 200 °C for 24 hours at 100 mTorr is on the right. Small mounds are smoothed out by the process.

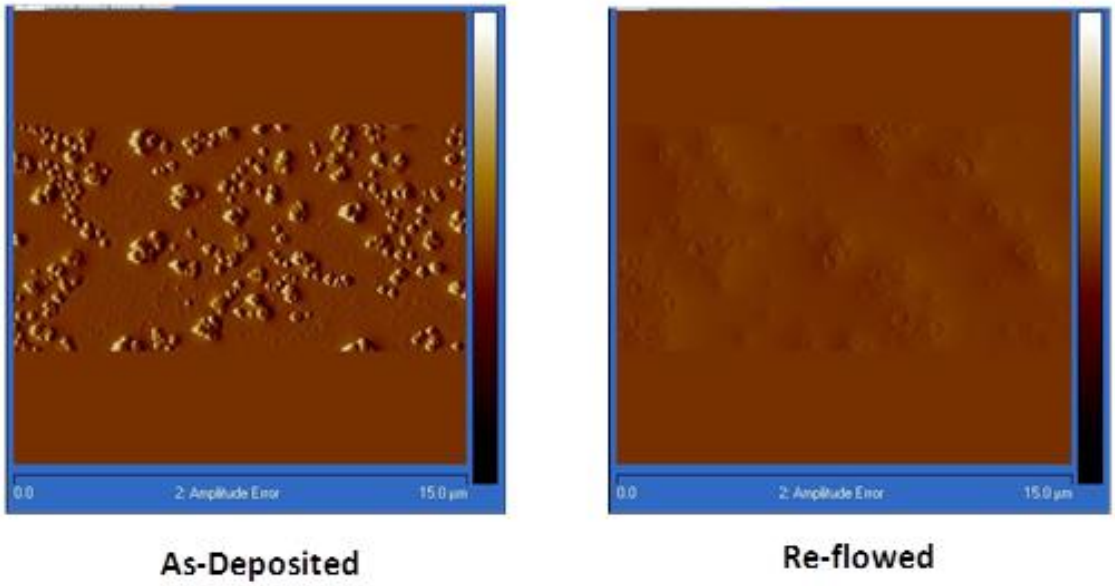

Figure 44. AFM roughness scans showing effect of annealing an as-deposited NRLP film at 200 °C for 24 hours at 100 mTorr. Small mounds are smoothed out by the process.

Ultimately the indicator for success of an ARC, annealed or not, is transmission. Transmission spectra of as-deposited and post-annealed NRLP ARCs are compared with the blank PC substrate transmission in Figures 45 and 46 respectively. Transmission of the as-deposited NRLP coating was generally worse over most of the visible spectrum than the blank PC flat. The as-deposited films are sufficiently antireflective, but the roughness of the coating degrades its transmission. Annealing efforts did improve transmission across the majority of the visible spectrum, even exceeding the transmission of the blank PC substrate. This can be seen in Figure 46. Improved transmission of an ARC as compared to the blank substrate can be considered a success for the project though the transmission data falls well short of the goals that were initially set.

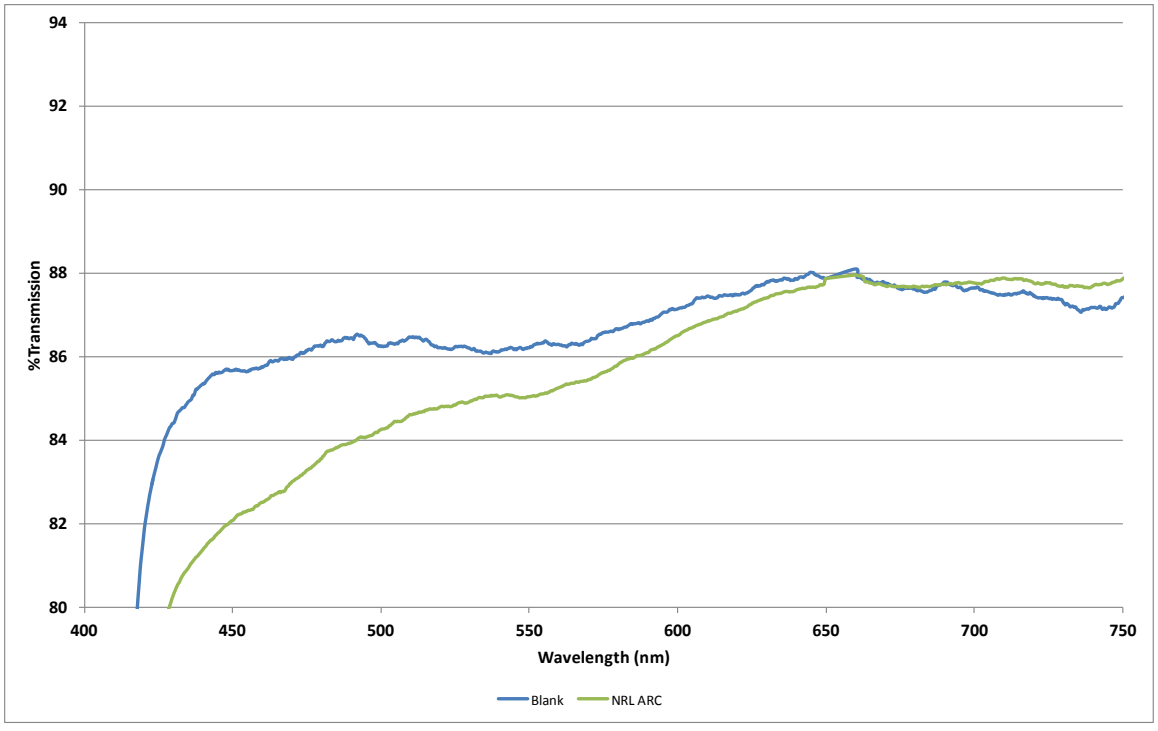

Figure 45. Transmission spectra of the NRLP-based AR coated PC window compared to an uncoated sample.

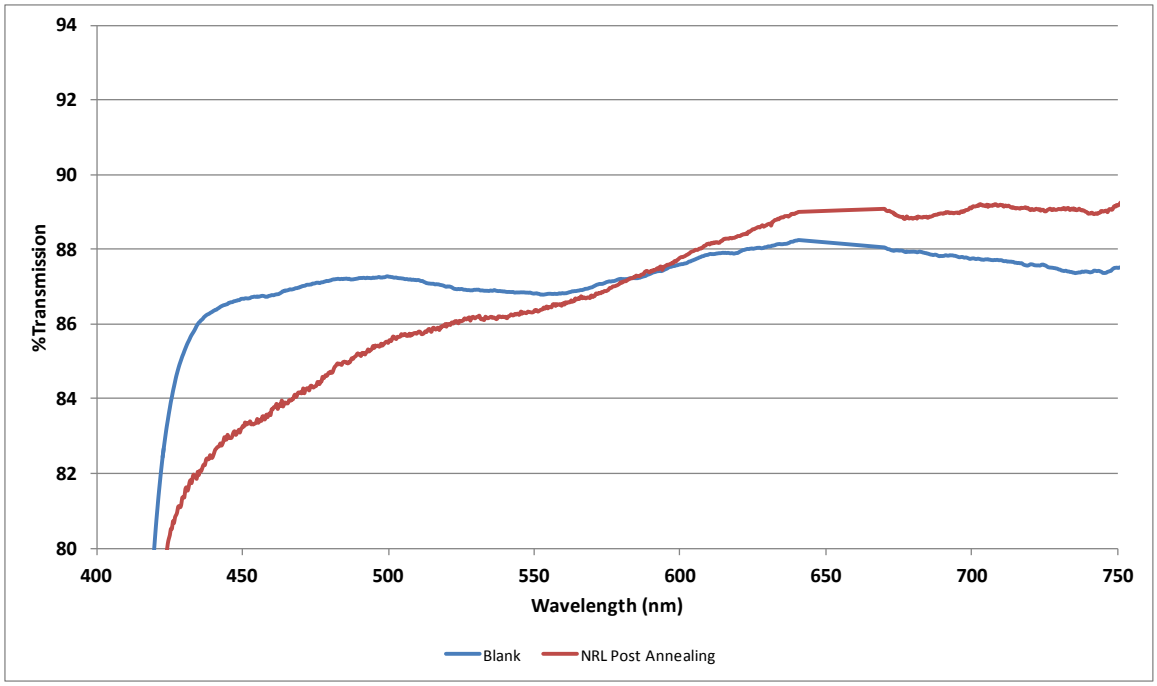

Figure 46. Transmission spectra of the NRLP-based AR coated PC window compared to an uncoated sample. This sample was reflowed at 200 °C at 100 mTorr for 24 hours. Note the improvement in transmission due to the smoothing of the film.

It is important to discuss the difference between a successfully antireflective coating and highly transmissive coating. An ARC can prevent reflection significantly while having poor transmission due to scattering or absorption of coating layers or the substrate. A fully transmissive coating will be sufficiently antireflective. The coatings produced by this study were successfully antireflective; however, due to scattering by coating roughness and absorbance by the PC substrates, the AR coated samples were not fully transmissive.

Environmental durability

The final necessary step to complete the project is to qualify the environmental durability of the mixed MAPLE and sputter coated antireflective coatings which adhered to the mathematical model. A lot of NRLP-ARC on PC samples were tested in accordance with Military Specifications MIL-C-48497A.[11] Tests included in this specification are adhesion testing, humidity testing, moderate abrasion, thermal stability, and solubility and cleanability. Adhesion testing was carried out using pieces of cellophane tape measuring approximately 1" by ½". The tape was pressed firmly against the coated surface, air bubbles were removed, and then the tape was quickly removed at an angle normal to the coated surface. The thin films were seemingly unaffected by this test. Subsequent to the adhesion test, samples were exposed to 100% humidity at 120°F for just over twenty-four hours. 100% humidity was achieved with a beaker of water being sealed in a polypropylene container with the samples, all of which were heated on a hotplate at 120°F. The samples were removed after the time period had elapsed and were cleaned with an optical wipe. All samples tested conformed to MIL-C-48497A sections 3.3.1 and 3.3.3 concerning physical appearance. The samples were not visibly altered by this test. Within twenty minutes of removal from the container, the samples were subjected to a moderate abrasion test which consisted of fifty strokes across their coated surface in straight overlapping lines. The abrader used was made from 100% cotton cheese cloth and conformed to size and apparatus specifications set by MIL-C-48497A. Samples retained no visible defects or marks after this abrasive test.

Thermal stability of the coatings was tested by exposure to high and low temperatures. Low temperature testing was carried out first. The specifications indicate

that the samples should reach a temperature of -80°F and be held within two degrees of that temperature for no less than two hours. The temperature change rate must not exceed 4°F per minute. These test parameters were met using a chloroform/LN2 slush bath. The melting point for chloroform is -82°F. Samples were placed in a glass dish that had thermal contact to a ceramic crucible that was inverted and placed into a room temperature chloroform bath. To monitor temperature, a K-type thermocouple was placed against the center of the glass dish with the samples surrounding it. The temperature of the bath was dropped slowly by adding small aliquots of liquid nitrogen into the chloroform. The purpose of the ceramic crucible was to allow for slow and even thermal conduction from the samples to the slush bath. The temperature was recorded per minute as the liquid nitrogen was slowly added and the solution began to freeze. The recorded rate of change was appropriate and within the given limits of the specifications. After two hours at -80°F $\pm$2°F, the samples were removed from the glass dish and allowed to equilibrate to room temperature. Once at room temperature, the samples were evaluated for physical appearance and subjected to a repeated moderate abrasion test. The samples had no blemishes or defects after these tests. High temperature test specifications prescribe a ramp rate of no more than 4°F per minute to a final temperature of 160°F which is held $\pm$2°F for two hours. These specifications were met using a Fisher Scientific convection oven with a digital temperature regulator. The samples were placed in a crystallization dish surrounding a K-type thermocouple fixed to the glass. The dish was placed in the center of a rack in the oven. Oven temperature settings were increased slowly and monitored by the thermocouple. Incremental increases in the temperature were recorded per minute and did not exceed the prescribed ramping rate. A temperature

of 160°F was reached and maintained for two hours. After being allowed to return to room temperature, the samples were examined for blemishes and subjected to another moderate abrasion test. The samples were unchanged by these tests.

MIL-C-48479A section 4.5.4.2 describes solubility and cleanability of the coatings. The specified solvents to be used are trichloroethylene, acetone, and ethyl alcohol. Our antireflective coatings are on polycarbonate substrates. Polycarbonate is soluble in both trichloroethylene and acetone. With this information, testing the coatings on this substrate with these solvents is not practical. The polymer chosen for the coatings, NRLP, is soluble in small alcohols and would not survive the ethyl alcohol treatment. No further solubility or cleanability testing were prescribed by the specifications. The tabulated results appear in Table 6.

Table 6. MIL-C-48497A environmental durability test results for the NRLP-based antireflective coating on polycarbonate substrates.

Test Qualifications	Sample 1	Sample 2	Sample 3	Sample 4	Sample 5
3.4.1.1 Adhesion					
Pass/Fail	Pass	Pass	Pass	Pass	Pass
3.4.1.2 Humidity					
Defects	Pass	Pass	Pass	Pass	Pass
Moderate Abrasion	Pass	Pass	Pass	Pass	Pass
3.4.1.3 Moderate Abrasion					
Defects	Pass	Pass	Pass	Pass	Pass
Optical	Pass	Pass	Pass	Pass	Pass
3.4.2.1 Thermal					
High Temp Defects	Pass	Pass	Pass	Pass	Pass
Low Temp Defects	Pass	Pass	Pass	Pass	Pass
High Temp Moderate Abrasion	Pass	Pass	Pass	Pass	Pass
Low Temp Moderate Abrasion	Pass	Pass	Pass	Pass	Pass

CHAPTER 5

CONCLUSION

In this study, a method of obtaining optical quality thin films for use as antireflective coatings (ARCs) for polycarbonate substrates was developed. The coatings were produced using a combination of Matrix Assisted Pulsed Laser Evaporation (MAPLE) deposition for polymer films and magnetron sputtering for dielectric films. MAPLE targets comprised of solvated Polymethylmethacrylate (PMMA), DuPont™ Teflon® AF (TAF), and a fluorinated polymer developed by the Naval Research Labs (NRLP). These targets were then evaluated in a series of designed experiments (DOE) to establish the deposition parameters that would produce the best optical quality films. The variables studied in the DOE included: matrix composition, polymer concentration in the matrix, and laser fluence. The measured responses for the deposited films were: thickness, uniformity, surface roughness, and defect density.

Prior to any depositions, the optical constants were independently measured for the three polymeric materials, and the dielectrics, SiO_2 and AlN, using spun-on polymer films and sputtered dielectric films on silicon substrates. The constants were used to mathematically model stacks of films that would result in the best ARCs for ophthalmic polycarbonate (PC) substrates. As a test for the models of the antireflective stacks, alternating layers of magnetron sputtered SiO_2 and spin coated Teflon® AF were deposited on a PC window. The experimentally obtained visible transmission spectrum

agreed with the model except the PC substrates absorbed more than the modeled PC. Front surface reflectance spectra of the coated PC window were in good agreement with the model and achieved the target reflectance of <0.5% over most of the 400-750 nm spectrum.

The development of the MAPLE process was the largest component of this project. The process used an Er:YAG laser emitting at 2937 nm to evaporate a solid target matrix of appropriately absorbing solvent depositing the desired polymer onto a substrate. The target and substrate were held in an inert atmosphere under vacuum. While the DOEs provided the best process parameters for obtaining the highest optical quality films, the best films were still significantly rough and caused scattering of incident light which decreased the total transmission below project goals. Process and matrix parameters were tailored to improve the film roughness with the best results being achieved by a post-deposition high temperature, vacuum reflow of the coatings.

ARCs containing each of the three polymers were deposited on polycarbonate blanks for final spectroscopic analysis. High quality films of PMMA and NRLP were obtained; however, TAF deposited as large polymer strands with no concise film due to solubility limitations. While significant antireflective properties were obtained with both PMMA and NRLP ARCs, the total project goals of <0.05% reflectance and >99.5% transmission were not reached. It is believed that the roughness of the as-deposited polymer films and inherent absorbance of the PC substrates are the cause for the negative results. The NRLP ARCs on polycarbonate substrates were tested under military specifications MIL-C-48479A for environmental durability. Specific tests were adhesion

strength, humidity stability, moderate abrasion resistance, thermal stability, and solubility. The samples passed all of the applicable tests for optical coatings.

Obtaining smoother, high optical quality films will be the focus of future studies. Methods to investigate include: employing a heated substrate holder to minimize solvent contamination and increase polymer flow during deposition to reduce roughness, investigating reflow techniques, and potentially combining multiple deposition steps into one system to maintain vacuum and reduce contamination.

LITERATURE CITED

1. Raut, H. K.; Ganesh, V. A.; Nair, A. S.; Ramakrishna, S. Anti-reflective coatings: A critical, in-depth review. *Energy Environ. Sci.* **2011**, 4, 3779-3804.

2. Harbecke, B. Coherent and Incoherent Reflection and Transmission of Multilayer Structures. *Appl. Phys. B* **1986**, 39, 165-170.

3. Tomlin, S. G. Optical reflection and transmission formulae for thin films. *Brit. J. Appl. Phys. (J. Phys. D.)* **1968**, 2, 1, 1667-1671.

4. Larouche, S.; Martinu, L. OpenFilters: open-source software for the design, optimization, and synthesis of optical filters. *Appl. Opt.* **2008**, 47, 1, C219-212.

5. Tec-Yam, S.; Rojas, J.; Rejón, V.; Oliva, A. I. High quality antireflective ZnS thin films prepared by chemical bath deposition. *Mater. Chem. and Phys.* **2012**, 36, 386-393.

6. Glaubitt, W.; Löbmann, P. Antireflective coatings prepared by sol-gel processing: Principles and applications. *J. Eur. Ceram. Soc.* **2012**, 32, 2995-2999.

7. Han, K.; Lee, H.; Kim, D.; Lee, H. Fabrication of anti-reflection structure on protective layer of solar cells by hot-embossing method. *Sol. Energy Mater. Sol. Cells* **2009**, 9, 1214-1217.

8. Bartzsch, H.; Lange, S.; Frach, P.; Goedicke, K. Graded refractive index layer systems for antireflective coatings and rugate filters deposited by reactive pulse magnetron sputtering. *Surf. Coat. Technol.* **2004**, 180-181, 616-620.

9. *CRC Handbook of Chemistry and Physics*, 94th ed.; Boca Raton, FL, **2013**.

10. Dumas, L.; Quesnel, E.; Robic, J.-Y.; Pauleau, Y. Characterization of magnesium fluoride thin films produced by argon ion beam-assisted deposition. *Thin Solid Films* **2001**, 382, 61-68.

11. Hong, E.; Byeon, K.; Park, H.; Hwang, J.; Lee, H.; Choi, K.; Jung, G. Y. Fabrication of moth-eye structure on p-GaN layer of GaN-based LEDs or improvement of light extraction. *Mater. Sci. Eng., B* **2009**, 163, 170-173.

12. Jiao, F.; Huang, Q.; Ren, W.; Zhou, W.; Qi, F.; Zheng, Y.; Xie, J. Enhanced performance for solar cells with moth-eye structure fabricated by UV nanoimprint lithography. *Microelectron. Eng.* **2013**, 103, 126-130.

13. Xu, H.; Lu, N.; Qi, D.; Gao, L.; Hao, J.; Wang, Y.; Chi, L. Broadband antireflective Si Nanopillar arrays produced by nanosphere lithography. *Microelectron. Eng.* **2009**, 86, 850-852.

14. Greer, J. A. Design challenges for matrix assisted pulsed laser evaporation and infrared resonant laser evaporation. *Appl. Phys. A* **2011**, 105, 661-671.

15. McCormick, R. D.; Lenhardt, J.; Stiff-Roberts, A. D. Effects of Emulsion-Based Resonant Infrared Matrix Assisted Pulsed Laser Evaporation (RIR-MAPLE) on the Molecular Weight of Polymers. *Polymers* **2012**, 4, 341-354.

16. Chrisey, D. B.; Piqué, A.; McGill, R. A.; Horwitz, J. S.; Ringeisen, B. R. Laser Deposition of Polymer and Biomaterial Films. *Chem. Rev.* **2003**, 103, 553-576.

17. Jelínek, M.; Remsa, J.; Kocourek, T.; Kubešová, B.; Schůrek, J.; Myslík, V. MAPLE activities and applications in gas sensors. *Appl. Phys. A* **2011**, 105, 643-649.

18. Piqué, A.; McGill, R. A.; Chrisey, D. B.; Leonhardt, D.; Mslna, T. E.; Spargo, B. J., Callahan, J. H.; Vachet, R. W.; Chung, R.; Bucaro, M. A. Growth of organic thin films by the matrix assisted pulsed laser evaporation (MAPLE) technique. *Thin Solid Films* **1999**, 355-356, 536-541.

19. Sellinger, A.T.; Martin, A. H.; Fitz-Gerald, J. M. Effect of substrate temperature on poly(methyl methacrylate) nanocomposite thin films deposited by matrix assisted pulsed laser evaporation. *Thin Solid Films* **2008**, 516, 6033-6040.

20. Mihaiescu, D. E.; Cristescu, R.; Dorcioman, G.; Popescu, C. E.; Nita, C.; Socol, G.; Mihailescu, I. N.; Grumezescu, A. M.; Tamas, D.; Enculescu, M.; Negrea, R. F.; Ghica, C.; Chifiriuc, C.; Bleotu, C.; Chrisey, D. B. Functionalized magnetite silica thin films fabricated by MAPLE with antibiofilm properties. *Biofabrication* **2013**, 5, 015007, 1-11.

21. Bloisi, F.; Barra, M.; Cassinese, A.; Rosario, L.; Vicari, M. Matrix-Assisted Pulsed Laser Thin Film Deposition by Using Nd:YAG Laser. *J. Nanomater.* **2012**, 395436, 1-9.

22. Johnson, S. L.; Appavoo, K.; Park, H. K.; Haglund Jr., R. F. Effects of laser wavelength, fluence, and pulse duration on infrared pulsed laser deposition of a conducting polymer. In *Photon Processing in Microelectronics and Photonics VII*; Ed. Holmes, A. S., **2008**, Proc. of SPIE Vol. 6879, 68790Y.

23. Pate, R.; Stiff-Roberts, A. D. The impact of laser-target absorption depth on the surface and internal morphology of matrix-assisted pulsed laser evaporated conjugated polymer thin films. *Chem. Phys. Lett.* **2009**, 477, 406-410.

24. Cowie, J. M. G.; Mohsin, M. A.; McEwen, I. J. Alcohol-water cosolvent systems for poly(methyl methacrylate). *POLYMER* **1987**, 28, 1569-1572.

25. Georgiou, S.; Koubenakis, A. Laser-Induced Material Ejection from Model Molecular Solids and Liquids: Mechanisms, Implications, and Applications. *Chem. Rev.* **2003**, 103, 349-393.

26. Vorm, O.; Roepstorff, P.; Mann, M. Improved Resolution and Very High Sensitivity in MALDI TOF of Matrix Surfaces Made by Fast Evaporation. *Anal. Chem.* **1994**, 66, 3281-3287.

27. Leveugle, E.; Zhigilei, L. V.; Sellinger, A. Fitz-Gerald, J. M. Computational and experimental study of the cluster size distribution in MAPLE. *Appl. Surf. Sci.* **2007**, 253, 6456-6460.

28. Hansen, C. Hansen Solubility Parameters: A User's Handbook. CRC Press, Inc., Boca Raton FL, **1999**. 208 pages.

29. Bubb, D. M.; Corgan, J.; Yi, S.; Khan, M.; Hughes, L.; Gurudas, U.; Papantonakis, M.; McGill, R. A. An experimental investigation of inhomogeneities in resonant infrared matrix-assisted pulsed-laser deposited thin polymer films. *Appl. Phys. A* **2010**, 100, 523-531.

30. Caricato, A. P.; Leggieri, G.; Martino, M.; Vantaggiato, A.; Valerini, D.; Cretì; Lomascolo, M.; Manera, M. G.; Rella, R.; Anni, M. Dependence of the surface roughness of MAPLE-deposited films on the solvent parameters. *Appl. Phys. A* **2010**, 101, 759-764.

31. Bubb, D. M.; Papantonakis, M.; Collins, B.; Brookes, E.; Wood, J.; Gurudas, U. The influence of solvent parameters upon the surface roughness of matrix assisted laser deposited thin polymer films. *Chem. Phys. Lett.* **2007**, 448, 194-197.

32. Kopecký, D.; Vrňata, M.; Vysloužil, F.; Myslík, V.; Fitl, P.; Ekrt, O.; Matějka, P.; Jelínek, M.; Kocourek, T. Polypyrrole thin films for gas sensors prepared by Matrix-Assisted Pulsed Laser Evaporation technology: Effect of deposition parameters on material properties. *Thin Solid Films* **2009**, 517, 2083-2087.

33. Sellinger, A.; Leveugle, E.; Fitz-Gerald, J. M.; Zhigilei, L. V. Generation of surface features in films deposited by matrix-assisted pulsed laser evaporation: the effects of the stress confinement and droplet landing velocity. *Appl. Phys. A* **2008**, 92, 821-829.

34. Department of Defense SBIR/STTR Archives. http://www.dodsbir.net/sitis/archives_display_topic.asp?Bookmark=39224 (accessed April 8, 2013).

35. Ng, A.; Li, C. H.; Fung, M. K.; Djurišić, A. B.; Zapien, J. A.; Chan, W. K.; Cheung, K. Y.; Wong, W. Accurate determination of the index of refraction of polymer blend films by spectroscopic ellipsometry. *J. Phys. Chem.* **2010**, 114, 15094-15101.

36. Teflon AF™ application guide from DuPont. http://www2.dupont.com/Teflon_Industrial/en_US/products/product_by_name/teflon_af/apps.html (accessed April 1, 2013).

37. Yang, M.K.; French, R. H.; Tokarsky, E. W. Optical properties of Teflon AF amorphous fluoropolymers. *J. Micro/Nanolith. MEMS MOEMS* **2008**, 7(3), 033010-1-033010-9.

38. Field, D. E.; Griffith, J. R. Cross-linked Fluoropolymer Coatings. *Ind. Eng. Chem., Prod. Res. Dev.* **1975**, 14, 1.

VITA

Jeff Simpson was born and raised in Abilene, TX. He received his high school education from Saint Stephens Episcopal School in Austin, TX. He then attended The University of Texas at Austin where he received a B.S. in Biology: Evolution, Ecology, and Behavior. Jeff lives in Austin with his wife, Molly.

Email address: JeffreyRSimpson@gmail.com

This thesis was typed by Jeffrey R. Simpson.